skb.se

SKB R-24-11

ISSN 1402-3091
ID 2052726
August 2025

Mapping geomorphological features in search of indications of glacially induced faulting along the Hudiksvall seismic cluster on the Bothnian coast using LiDAR imagery

Christian Öhrling
Geological Survey of Sweden

Keywords: Postglacial faulting, Paleo seismicity, LiDAR, Glacially-triggered faulting, Earthquake-triggered landslides

This report concerns a study which was conducted for Svensk Kärnbränslehantering AB (SKB). The conclusions and viewpoints presented in the report are those of the author. SKB may draw modified conclusions, based on additional literature sources and/or expert opinions.

This report is published on www.skb.se

Abstract

This study presents a geomorphological analysis aimed at identifying indications of glacially-triggered faulting along the 'Hudiksvall-seismic cluster' on the Bothnian coast. The redistribution of tectonic stress during the advance and retreat of continental ice sheets can trigger seismic reactivation of faults. Understanding how, when, and where these events occur is important for predicting the stability of structural bedrock blocks. This knowledge is particularly relevant to the construction of the final repository for spent nuclear fuel in Sweden, which is managed by SKB, the Swedish Nuclear Fuel and Waste Management Company.

The study utilizes data from the modernized and expanded Swedish National Seismic Network (SNSN), which has provided a massive increase in the number of detected and analyzed earthquakes in Sweden since the year 2000. This data reveals a cluster of high seismic activity around Hudiksvall. The primary background data used for this study is 1 m resolution national elevation model in the form of a digital elevation model (DEM), derived from airborne Light Detection and Ranging (LiDAR) data. The geomorphological criteria that we searched for were scarps that crosscut glacial deposits. Further, landslide scars have been mapped and the distribution can be correlated to known or suspected glacially-triggered faults.

Three hundred scarps were mapped, of which four sites are particularly interesting. Most of the digitized lines represent distinct scarps in postglacial sand, bedrock faults without indications of postglacial ruptures, or subglacial meltwater features. The identified scarps of interest are here proposed to be subjected of in-depth studies, and selections of locations for trenching in the field.

Sammanfattning

Denna studie består av en geomorfologisk analys som syftar till att identifiera indikationer på glacialt utlösta förkastningar längs det 'seismiska Hudiksvallsklustret' på Bottenvikskusten. Under framryckning och retirering av inlandsisar kan omfördelning av tektoniska spänningar bygga upp och utlösa seismisk reaktivering av förkastningar.

Att förstå hur, när och var dessa händelser inträffar är viktigt för att förutsäga stabiliteten hos strukturella berggrundsblock. Denna kunskap är särskilt relevant för uppförandet av slutförvaret för använt kärnbränsle i Sverige, som förvaltas av SKB, Svensk Kärnbränslehantering. Det moderniserade och utökade svenska nationella seismiska nätverket (SNSN), har gett en massiv ökning av antalet upptäckta och analyserade jordbävningar i Sverige sedan år 2000. Dessa data avslöjar ett kluster av hög seismisk aktivitet runt Hudiksvall.

De primära bakgrundsdata som används för denna studie är en nationell höjdmodell med 1 m upplösning i form av en digital höjdmodell (DEM), härledd från flygmätningar med *Light Detection and Ranging* (LiDAR). De geomorfologiska kriterierna som vi använder vid sökningen är linjära brytningar (branter) i landskapet som korsar glaciala avlagringar. Vidare har skredärr kartlagts och fördelningen av dessa kan korreleras till kända eller misstänkta glacialt inducerade förkastningar (*glacially triggered faults,* GTF). Tre hundra branter kartlades, varav fyra platser är särskilt intressanta. De flesta av de digitaliserade linjerna representerar distinkta bryt i postglacial sand, berggrundsförkastningar utan indikationer på postglaciala brott eller subglaciala smältvattenerosion. De identifierade branterna av intresse föreslås här bli föremål för djupgående studier och urval av platser för grävning i fält.

Contents

1 Introduction

The advance and retreat of continental ice sheets redistribute tectonic stress which may, under certain circumstances, trigger seismic reactivation of faults. The knowledge of how, when, and where these occur is crucial for the prognostication of stability of structural bedrock blocks. This subject plays an important role for the construction of the final repository of spent nuclear fuel in Sweden; managed by SKB, the Swedish Nuclear Fuel and Waste Management Company.

A massive increase in the number of detected and analysed earthquakes in Sweden has been provided through the modernization and expansion of the Swedish National Seismic Network (SNSN) since the year 2000. Since the start of automatic processing in August 2000 more than 10,700 earthquakes have been detected and located, with magnitude and focal mechanism determinations (Lund et al. 2021). This can be compared with the approximately 1,400 Swedish earthquakes recorded between 1375 and 2000 in the joint Nordic earthquake catalogue – FENCAT (Ahjos and Uski 1992, Oinonen et al. 2021).

This study was a desktop study, with the exception of one and a half days of field visits to a few scarps. To assess whether the identified scarps are glacially-triggered faults, firstly, they need to be examined in the field, secondly, they need to be trenched.

1.1 Purpose

The data from the SNSN reveals a cluster of high seismic activity around Hudiksvall (Figure 1-1). The purpose of this study is to search for indications of glacially triggered faulting in an area covering this cluster. Identified structures are intended to be studied on-site and, if necessary, applied for excavation for sedimentological studies. The work was ordered, from the Geological Survey of Sweden (SGU), by SKB and is part of a larger SKB funded project investigating the swarm of seismic events in the area.

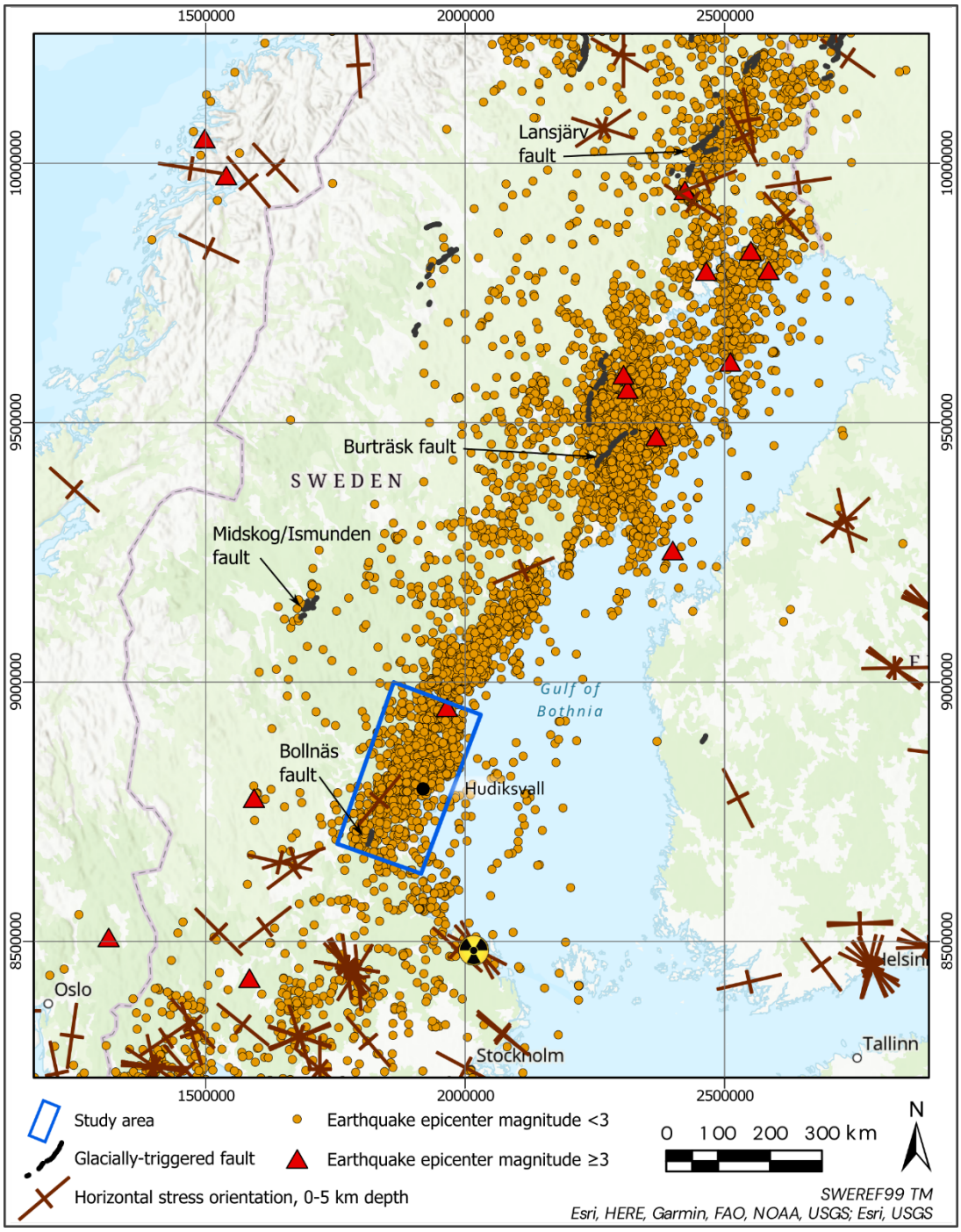

Figure 1-1. *Map of central-northern Sweden. Fault scarps, represented by black lines are downloaded from the International database of glacially induced faults (Munier et al. 2020). The faults at Bollnäs and Midskog/Ismunden (Jämtland) are mentioned in the text. The earthquake data from the Swedish National Seismic Network represent a monitoring period from 2000 until present (Lund et al. 2021). The horizontal stress data are from the world stress map, and selected information are from the upper 5 km of the earth crust (Heidbach et al. 2016). Forsmark, the site chosen for the construction of the final repository of spent nuclear fuel, is represented by a black and yellow radiation symbol.*

2 Geological setting and background

The study area, defined by SKB, at the east coast of Sweden is c. 13 000 km^2 of which 3380 km^2 is below the Baltic Sea. It covers large parts of the county of Gävleborg and a smaller part of southern Västernorrland county (Figure 1-1). The landscape is the result of geologic processes during different geologic periods. The most spectacular formation in the area is probably the Dellen crater (Figure 2-1), caused by a meteorite impact 140,82 ± 0,51 Ma (Mark et al. 2013). Further, there are re-exposed denudation surfaces in terms of the so-called sub-Cambrian peneplain, the uplifted and eroded sub-Cambrian peneplain and the sub-Mesozoic hilly relief (Figure 2-1B, (Lidmar-Bergström and Olvmo 2015). During the Mesozoic Era the climate was moist and warm, which triggered intensive deep weathering. Through the Paleogene and Neogene Periods erosional processes caused uplift of varying extent around the Scandinavian peninsula; coastal plains, residual hills and most of the large river valleys took shape during this time (Grånäs 2010). The glacial surficial deposits have, with few exceptions, been deposited during deglaciation. Postglacial deposits include lacustrine- and fluvial sediments, wave-washed sediments, aeolian sediments and peat.

2.1 Bedrock

The majority of the bedrock in the study area belong to the 2.0-1.8 Ga Svecokarelian orogen (Högdahl and Bergman 2020, SGU 2022, Skyttä et al. 2020). Subunits include the Ljusdal lithotectonic unit and the Bothnia-Skellefteå lithotectonic unit (Figure 2-1A). East of the coastline, still below the Bothnian Sea, the predominate sedimentary cover rocks are Mesoproterozoic and Paleozoic (Figure 2-1).

The Ljusdal lithotectonic unit is separated from the Bothnia-Skellefteå lithotectonic unit, to the north by the Hassela Shear Zone (Sjöström et al. 2000). To the west and south, the Storsjön-Edsbyn Deformation Zone (Bergman et al. 2006) and the Hagsta Gneiss Zone (Bergman and Sjöström 1994, Högdahl et al. 2009) separates the Ljusdal unit from the Bergslagen lithotectonic unit. Dextral movement was dominant in the deformation zones, but dip-slip movement was also important in especially the Storsjön-Edsbyn Deformation Zone (Bergman and Sjöström 1994).

The highest horizontal stress in the area is NW-SE, and the lowest SW-NE (Figure 1-1, (Heidbach et al. 2016). Thereby, the deep, open bedrock fractures occur parallel to the Bothnian coast. Fractures not parallel to the coast will more likely be shear fractures (Moon et al. 2020).

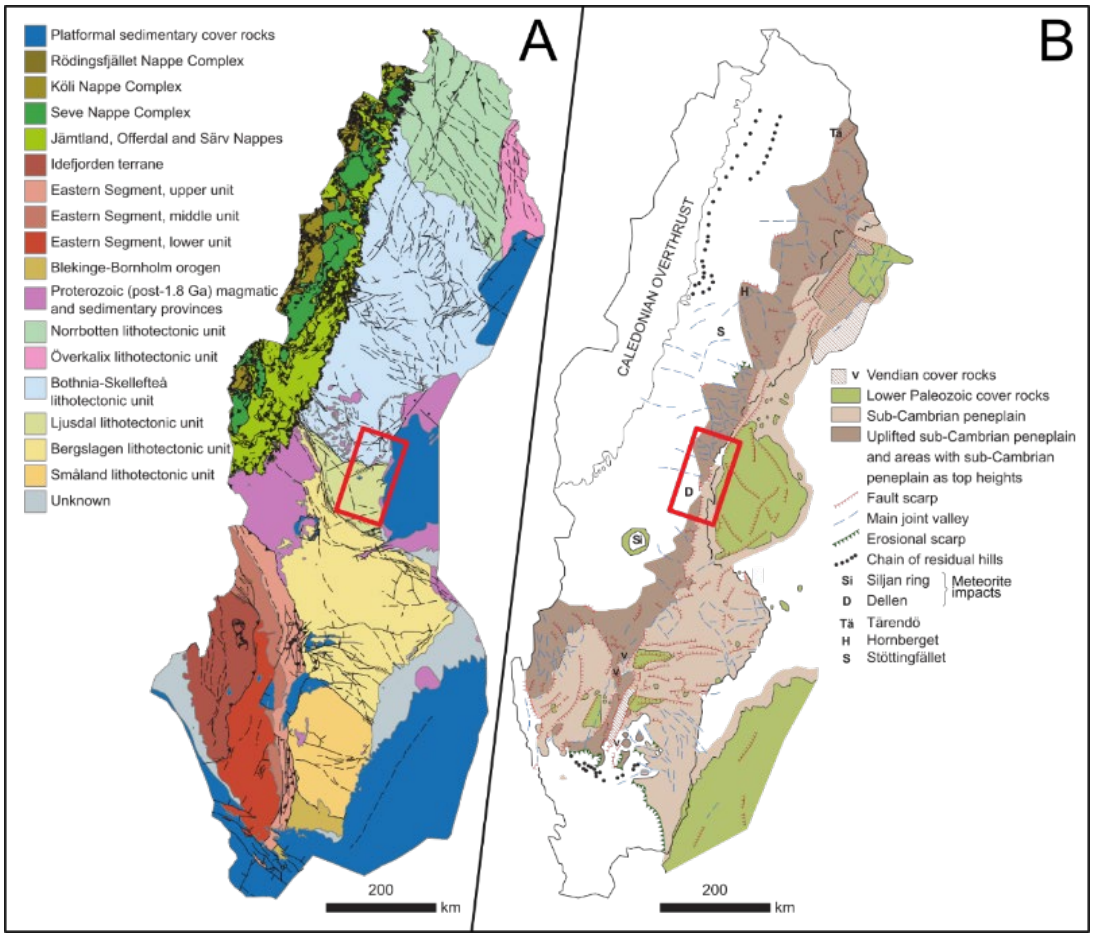

Figure 2-1. *A) Lithotectonic units in Sweden, based on Bergman et al. (2012), modified by Grigull et al. (2019). B) The extent of the sub-Cambrian peneplain and the sedimentary cover rocks; figure from Lidmar-Bergström and Olvmo (2015). Letter D marks the Dellen impact structure. The study area in eastern Sweden is marked with the red rectangle.*

2.2 Late Weichselian Ice Sheet retreat and the Holocene epoch

The Scandinavian Ice Sheet rapidly melted away (c. 300-400 m per year) from the area approximately between 10 500 and 11 000 cal. years BP (Berglund 2004, 2005, Hughes et al. 2016). Due to the damming ice sheet, glacial rebound and topography, the Baltic basin underwent four major stages during deglaciation; The Baltic Ice Lake (16 000–17 000 cal. years BP), the Yoldia Sea (11 700–10 700 cal. years BP), the Ancylus Lake (10 700–9 800 cal. years BP), and The Littorina Sea (9 800–present). For a comprehensive review of the development of the Baltic basin under the Quaternary period see Andrén et al. (2011) and the references therein. The general ice-flow direction in the study area is from the northwest. However, the details are more complex, which is manifested by the glacial striations and -lineations in Figure 2-2. Due to glacial isostatic adjustment the area was depressed by the Scandinavian Ice Sheet. This caused a high stand of water along the coast. The highest coastline in the study area is 270 m.a.s.l. in the northern part, and c. 230 m.a.s.l. in the southern part. The glacial isostatic rebound is still causing land uplift with c. 7-8 mm/year. The subsequent isostatically induced regression results in a constant drying of new land areas. The significance of this is considerable since the wave action during land uplift redistributes sediment leading to erosion of geomorphic landforms.

When the glacial ice in the Bothnian basin broke up, icebergs transported and deposited debris on what today is the coastal plains. Consequently, boulders of Paleozoic rocks are found on several terrestrial locations with a provenance from the bottom of the Bothnian Sea (Lundqvist 1963). Recently, with detailed elevation data, the geomorphic evidence, fossil pits and scrapes, of an armada of icebergs is clearly seen along the coast from Stockholm to Sundsvall (Öhrling et al. 2018, 2019). De Geer (1929) interpreted the geological record to show that the suggested fast marine-ice retreat in the area must have caused a massive production of icebergs. Further, Greenwood et al. (2015, 2017) present a glacial geomorphological data set showing a Bothnian-ice stream, with an onset in terrestrial Sweden, south of Umeå. The glacial landforms indicate the breakup of this ice stream c. 80 km north of Forsmark (Greenwood et al. 2017). The event is assumed to account for the transportation of limestone as ice-rafted detritus (IRD), which has been reported as spots of lime in a c. 150-year interval within the varve record in the southern part of the study area (e.g. Strömberg 1989). Later, when only sea ice remained in the Bothnian bay, the ice sheet confined to the northern coastal zones would oscillate and calve. Sediment records in large parts of the north Atlantic Sea floor show evidence of periods with high fluxes of IRD from eastern Canada. These events, called Heinrich events, generally occurred during stadial glacial conditions (colder periods) (Heinrich 1988, Hemming 2004). There is no clear consensus over the cause of formation of these events, or layers (Haapaniemi et al. 2010). Most theories are coupled to climate change in some way, which affected the Laurentide Ice Sheet in such a way that massive calving events occurred. One of the hypotheses, however, is that they could have been caused by glacially induced seismicity (Hunt and Malin 1998); i.e. earthquakes cracked the ice margin open, releasing a high concentration of debris-laden icebergs.

The deglacial landscape consists of landforms and sediments deposited or eroded by glacial ice and glacial meltwater. When the Scandinavian Ice Sheet had disappeared, other processes took over; these include wave washing, weathering and deposition of organic material. Hence, the geomorphology that can be analyzed in search of indications of late- or postglacial faulting by remote sensing is glacial landforms (e.g. till plains, moraines, drumlins, eskers, outwash surfaces) and postglacial landforms (e.g. shorelines, raised beaches, dunes, landslide scars, debris fans, peat bogs, deltas).

Claims of strong paleoseismicity (several earthquakes of magnitude >M8) around the peninsula east of Hudiksvall (Hornslandet) has been reported (Mörner 2003, 2004, 2011, 2013). However, there are several contradictions in these interpretations and alternative explanatory models have been proposed (Carlsten and Stråhle 2000, Lagerbäck and Sundh 2008, Wänstedt, 2000). Mörner (2004) claimed evidence for paleoseismicity, in this area, are summarized from forty-seven sites with bedrock dislocations, fourteen sites of sediment liquification, and thirteen sites of tsunami deposits (Figure 2-2).

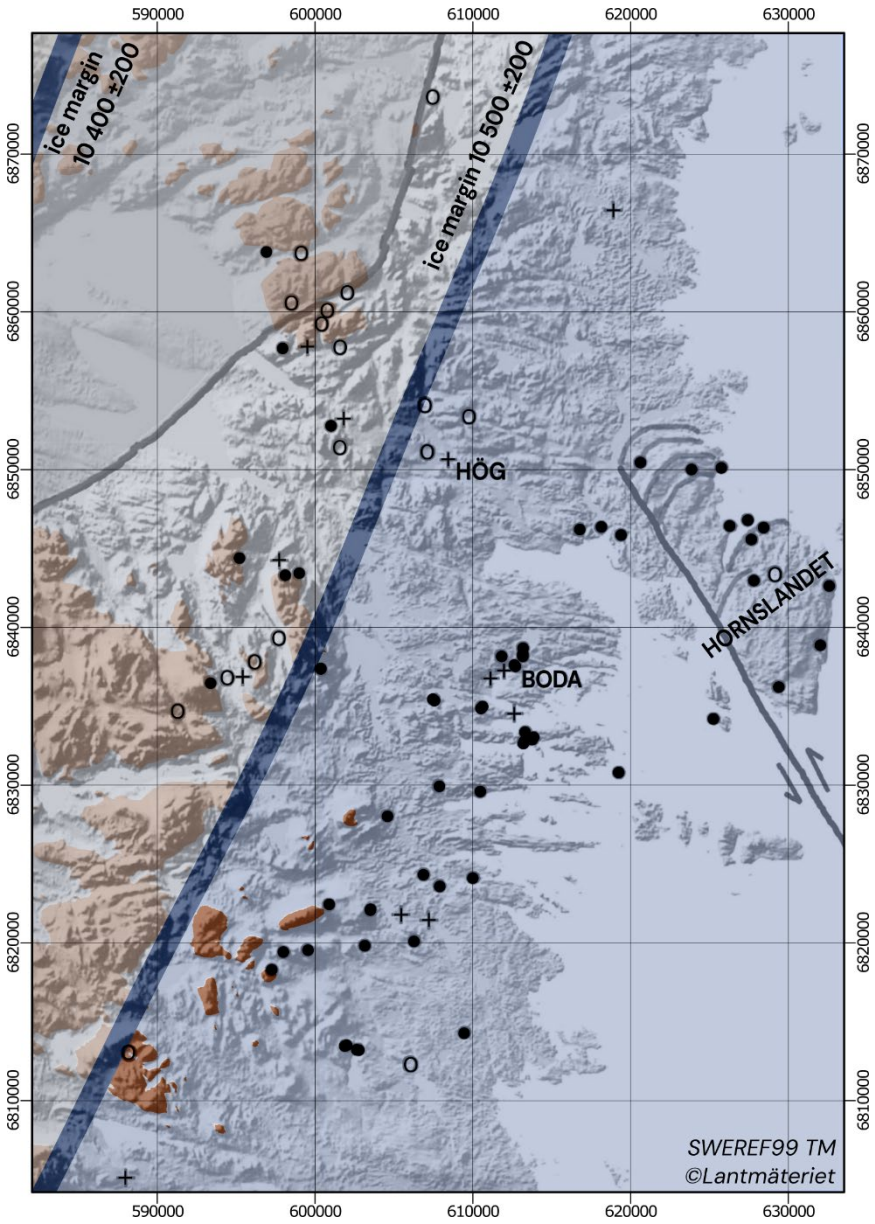

Figure 2-2. *Deglaciation of the Hudiksvall area, thick blue lines represent the receding ice margin. Red-brown areas are the uplifted land areas during this time. Mörner (2004) claims evidence for paleo seismicity from forty-seven sites with bedrock dislocations (black dots), fourteen sites of sediment liquification (plus signs), and thirteen sites of tsunami deposits (open circles). Modified from Mörner (2004).*

2.3 Glacially-triggered faults

Glacially-triggered faults (GTF), previously often called postglacial faults, are faults that are known or suspected to have been re-activated due to a combination of tectonic and isostatic stresses during or shortly after deglaciation. Recently however, dating of paleo-seismic events suggests several episodes, with spans from the beginning of the Weichsel glaciation (Sutinen & Middleton 2021) to less than 600 years ago (Olsen et al. 2021). Scarps that cut across (de-)glacial landforms or sediments suggest that they are younger than the glacial deposits (i.e. post-glacial).

Within the study area, there is one fault line previously recognized (Munier et al. 2020), the Bollnäs fault (Figure 1-1; (Malehmir et al. 2016, Mikko et al. 2015, Smith et al. 2014). GTFs are known to exist in central Jämtland, see Figure 1-1, but mostly further north (e.g. *Burträsk, Lansjärv, Pärvie*). For further details on GTFs in Northern Europe, see Steffen et al. (2021) and more specifically in Sweden, Appendix 1 in Lund et al. (2017) and references therein.

Despite the lack of known scarps, paleo-seismic events have also been proposed in the Hudiksvall area. Mörner and Sjöberg (2018) maintain the neotectonic origin for several boulder caves in the area. However, Hall et al. (2020) convincingly present how these caves formed through 'glacial ripping'; a bedrock-disruption process of subglacial hydraulic jacking, ripping, and glacial transport. Mörner (1996, 1999, 2004) suggests that several observed sediment stratigraphies with liquefaction and varve deformation (including the plus signs in Figure 2-3) represent the actions from paleo-seismically induced tsunamis. These claims are discredited by Smith and Öhrling (2022) where they show that the evidence is deficient.

2.4 Earthquake-triggered landslides

Most stronger earthquakes (magnitude >4) trigger landslides which can be of all types, though all types of landslides can also occur without a trigger from crustal movement (Jibson 2012, Keefer 2002). Yet, landslide scars are commonly used to study areas of postglacial seismicity in deposits that are less prone to sliding under normal conditions (Kujansuu 1972, Lagerbäck and Sundh 2008, Sandersen and Sutinen 2021, Stewart et al. 2000, Sutinen et al. 2009). Coarse and/or poorly sorted sediments are such deposits; 'debris' in Varnes classification of landslides (Varnes 1978). When masses slide down slope, other deposits further down, get covered. This means that the timing of earthquakes (minimum ages) can be determined through buried datable material such as alluvial or lacustrine deposits and peat. Ojala et al. (2018) reports radiocarbon dates from several landslides, which are suggested to relate to GTFs. Their results show that the seismic events occurred in intervals; the majority between 11 000 and 9 000 cal. years BP, then some between 6000 and 5000, and some between 3000 and 1000 cal. years BP. Landslides caused by earthquakes commonly occur within a radius of 35-40 km from the epicenter (Keefer 2002, Ojala et al. 2019a). Keefer (1984) analyzed data from 40 historical earthquake-triggered landslide areas and classified seismically triggered landslides into three major categories: steep slope 'disrupted slides', moderate slope 'coherent slides', and gentle to very low-angle slope 'lateral spreads and flows'. Consequently, 'low-angle slope' is often used as an argument in favor of a seismic trigger of a pre-historic landslide. It is easier to imagine other triggers on steeper slopes, whilst the liquefaction of, for example, till on very low angles is assumed to require shaking ground movements (e.g. Mangerud et al. 2018).

However, landslides in coarse sediment can be triggered by other mechanisms, like extreme weather events such as heavy rain (Crosta and Frattini 2008, Dai et al. 2003), as seen for example in the year 2000 along the glacial till slopes of *Indalsälven* (Grånäs 2010), just outside the study area. Landslide scars are also a common phenomenon below paleo-shorelines, such as the highest coastline, where the sediment saturation and pore pressures change during regression (e.g. Smith et al. 2017). Landslides in till also occur in periglacial environments, where the presence of permafrost influenced by freeze/thaw cycling causes sliding on moderate slopes (e.g. Lissak et al. 2020). The scientific interest in this type of thawing-permafrost (thermokarst) landslides has increased in recent years, mostly because of their correlation to climate warming and feedback of carbon emissions (Douglas et al. 2021, Farquharson et al. 2019, Lewkowicz and Way 2019). In the study area there are, albeit no records of permafrost since the deglaciation.

The terrestrial landscape unveiled by the receding ice sheet lost their ice support, were unvegetated and possibly water saturated. Thus, this so called paraglacial environment constitute a period of time when glaciated landscapes effectively respond to non-glacial conditions (Slaymaker 2009). Glacial sediments are during these periods more responsive to disturbances.

Further, all these landslide types, induced by heavy rain, changing pore pressures, warming, thawing etc. can also have been triggered in combination with seismicity (Lissak et al. 2020).

2.5 Fractured bedrock and boulder dislocation

In several places within the study area, so-called *boulder caves* occur. These are boulders spread along a rock slope. The most well-known of these features are the 'Boda Caves' near Iggesund, south of Hudiksvall (Figure 2-3). Although it has been proposed that the caves resulted from large postglacial earthquakes, cracking the bedrock (Agrell 1981, Mörner 2004, Sjöberg 1986), the more commonly accepted explanation is that the boulders have been eroded and transported by the Scandinavian Ice Sheet (Hall et al. 2020, Lagerbäck et al. 2005, Lagerbäck and Sundh 2008).

Another geomorphic feature that can support a GTF interpretation, is groundwater seepage (springs) along suspected scarps; 'recently' fractured bedrock leak and then heal with time (Hanson et al. 1999, Lagerbäck and Sundh 2008).

3 Methods and material

SGU uses geomorphological mapping as part of the workflow in making Quaternary maps (Karlsson et al. 2021). In this study the aim is to map lineations that cross-cut glacial sediments or landforms. With few exceptions, the methods employed in this study are identical to what was applied and described in Mikko et al. (2015) and Öhrling et al. (2018). The ESRI software ArcGIS ArcMap was exchanged in favor of ESRI ArcGIS Pro and a few digital elevation model (DEM) derivatives were added or removed. The general workflow is presented in Figure 3-1.

3.1 Spatial data

The primary background data used for this study is a 1 m resolution national elevation model in the form of a digital elevation model (DEM), derived from airborne Light Detection and Ranging (LiDAR) data. Öhrling et al. (2018) obtained a 1 m DEM from the point cloud data behind the 2 m national elevation data, but since late 2020 there is a 1 m DEM provided by Lantmäteriet (Lantmäteriet, 2021); in this study the latter was used. All data have been processed and presented using the SWEREF99 TM coordinate reference system, which is the standard projection system used in Sweden for mapping and spatial data. Most data sets were prepared with the software ESRI ArcGIS Pro 2, while 'curvature' and 'TPI' were managed with GRASS and GDAL tools within QGIS (QGIS.org 2022).

3.2 Mapping procedure

Lineaments and scarps were mapped manually, and most mapping and analysis of data were performed using ArcGIS Pro 2.

The approach to screen the assigned area was to first render a grid that was used to keep track of which areas were checked, and which were not. Then each grid cell was screened for lineaments and scarps, starting with a zoom scale of approximately 1:15 000 and then zooming in on suspect lineaments (often in about 1:4 000). To get a better picture of the regional context it is needed to zoom out as well, to about 1:30–50 000. During this process, the different background-datasets were switched between.

Scarps were identified as linear scarps that crosscut, and potentially displace, glacial landforms and/or sediments. Scarp features were mapped as polylines and stored in an ESRI shapefile. Simultaneously, landslide scars were identified as arcuate or linear features facing down slope and mapped as polylines in a separate shapefile.

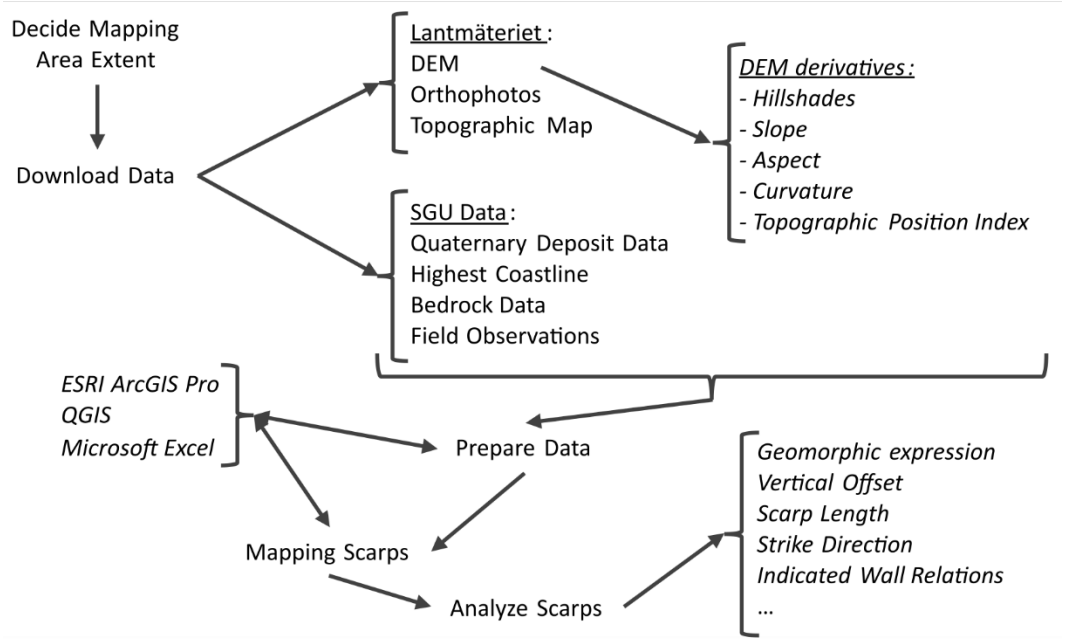

Figure 3-1. *Method workflow diagram.*

4 Results and interpretations

Three hundred scarps were mapped in this study. Most of them were caused by processes other than postglacial fault ruptures, such as old bedrock faults, glaciofluvial erosion, or excavators. Figure 4-1 shows the location of the scarps that are mentioned in the text, together with landslide scars mapped in this study.

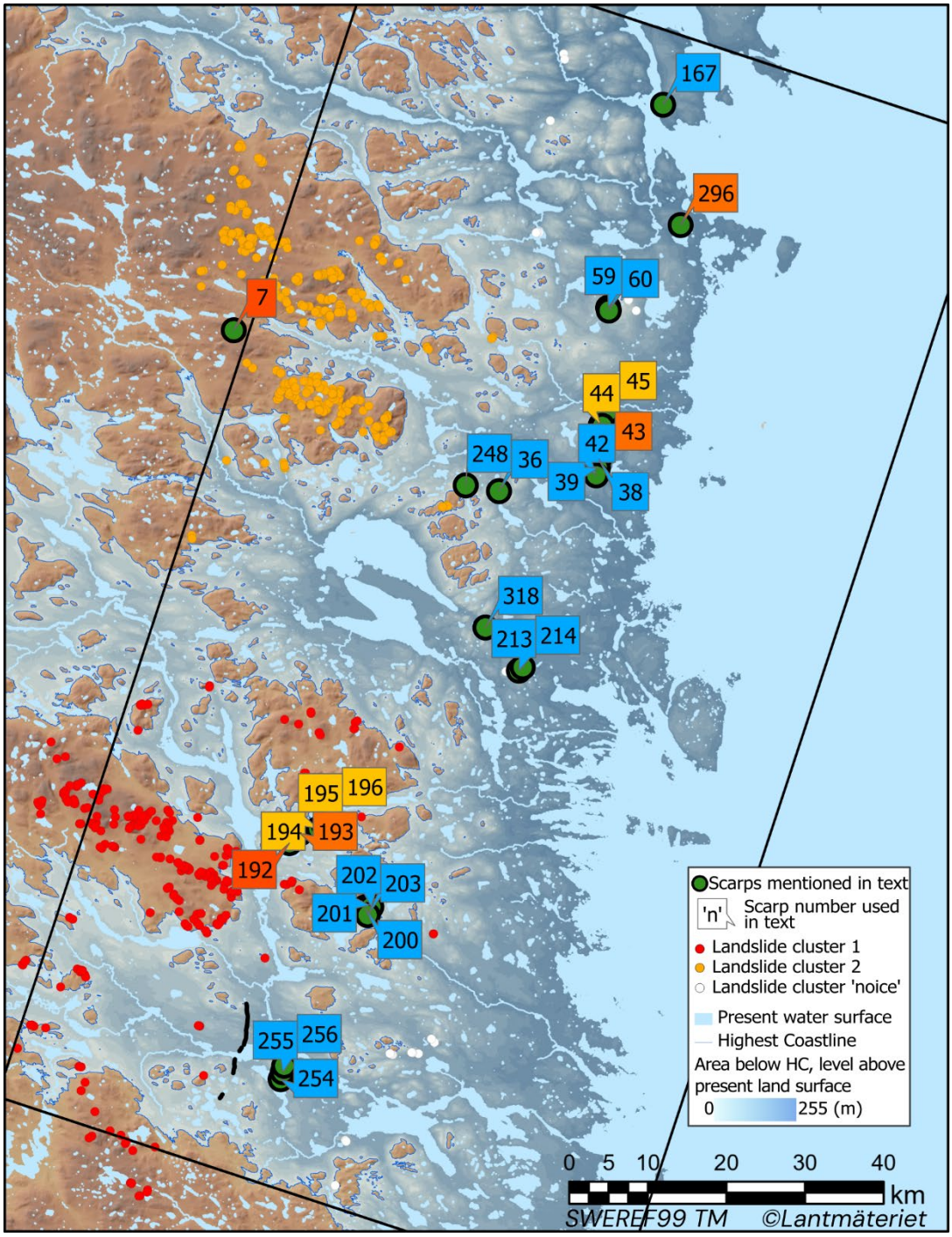

Figure 4-1. *Overview figure showing the location of the scarps that are mentioned in the text. Blue text boxes represent scarps in Figure 4-2 to 4-6. Red, orange, and yellow text boxes represent the scarps in section 4.2, and Figure 4-7 to 4-11. The landslide clusters are represented by red and yellow dots; described in more detail in section 4.3.*

4.1 Examples of non GTF scarps

Below are a few selected examples of mapped scars that are interpreted as caused by other processes. The numbers refer to the supplementary shapefile.

4.1.1 Distinct scarps in postglacial sand

Scarp 288, which was visited during fieldwork, is c. 700 m long, strikes E-W, and faces south (Figure 4-2). At the eastern end there is a small spring flow. The scarp is located close to the Hög gravel pit, which is a site investigated regarding paleo-tsunamis in the area (Mörner 1999, Smith and Öhrling 2022). However, the interpretation is that the scarp formed by several fluvial processes and not by a postglacial earthquake. The scarp is proposed to be eroded into a glaciofluvial subaqueous fan deposit. The fan is interpreted to have been formed by the same glaciofluvial system as the Hög subaqueous fan (Figure 4-2). When the relative sea level fell, shorelines formed. At one stage the environment developed from an open passage (strait) for longshore drift, to the closing and dramatically shifting of the sediment transportation and deposition. These events caused the formation of the distinct scarps (Figure 4-2, inset).

Scarp 167 was also visited during fieldwork. It is a 370 m long, NNE–SSW trending and W facing scarp that appears to crosscut paleo-shorelines (Figure 4-3). Small pits in the scarp reveal sand and gravel with rounded cobbles. There is a trail along the foot of the scarp. On the eastern side, above the scarp, there is an old sand pit (orange shading in Figure 4-3). The interpretation is that the scarp has been formed by fluvial erosion through wave action and sediment drift.

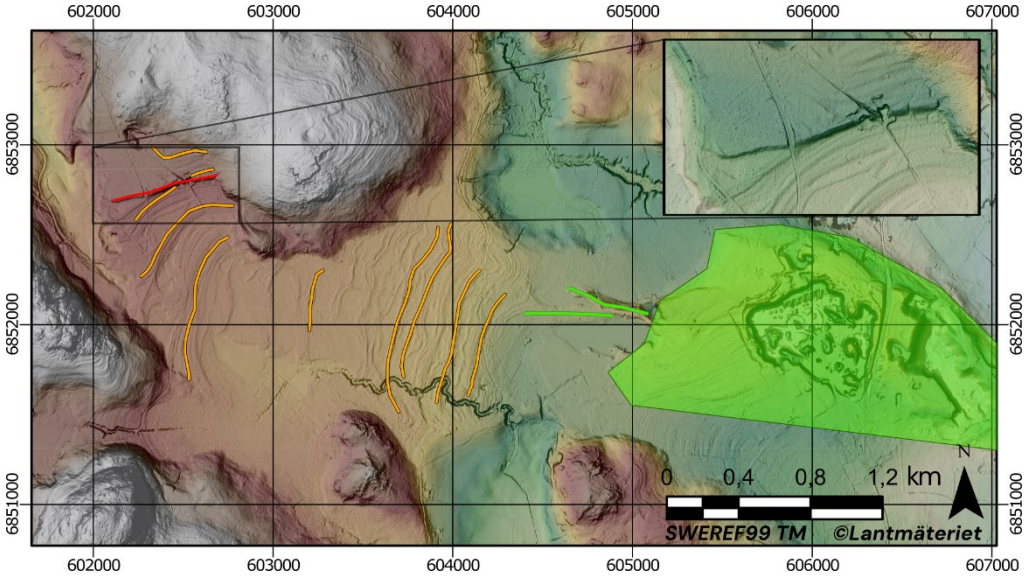

Figure 4-2. *Scarp no. 288 (red line and inset) is located on an outwash surface that is interpreted to pe part of the same glaciofluvial system as the Hög gravel pit (green polygon). Green lines represent feeding eskers, and the orange lines represent raised shorelines. The scarp is interpreted to have formed by fluvial processes when the sea strait closed during relative sea level drop, which changed the currents, sediment transport and erosion patterns.*

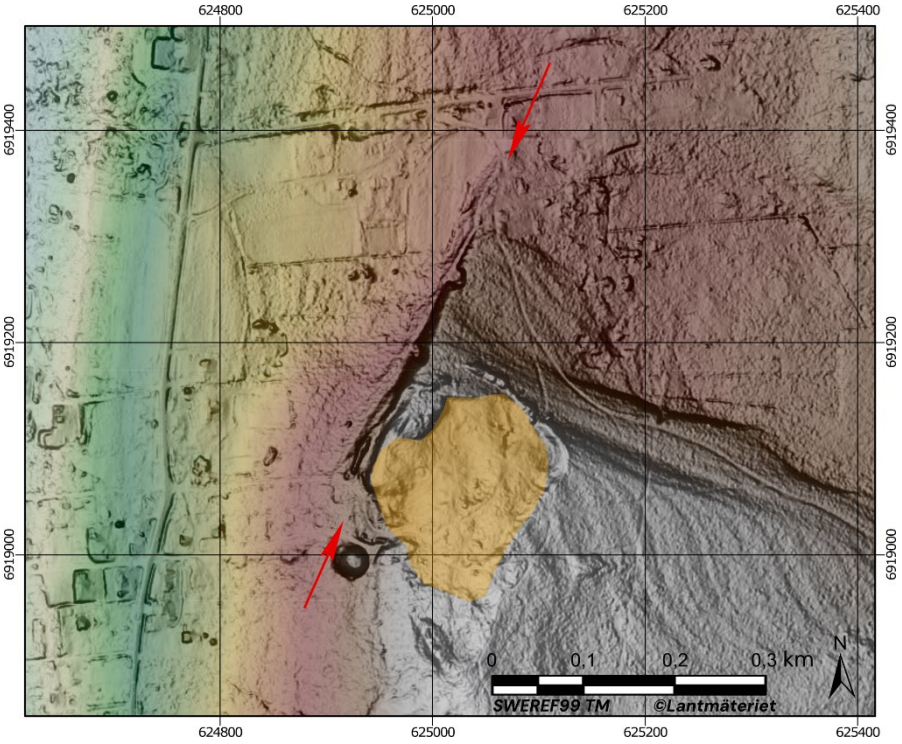

Figure 4-3. *Scarp no. 167 appear to crosscut shorelines. The yellow polygon represents a closed and restored sand pit. The formation is not fully understood, but it is interpreted to be the result of fluvial erosion during relative sea level drop.*

Scarp 36 is a 700 m long scarp, which strikes SW-NE and faces towards the NW (Figure 4-4). A field visit revealed a boulder rich scarp. The south and east slopes have clear paleo shorelines. On the eastern side above the scarp, there is a gravel pit showing 10 m thickness of gravelly sand. Parallel to the scarp, at the SW end, a spring discharge. No signs of cut shorelines can be found. The interpretation of the scarp is to have been formed by fluvial erosion and wave action.

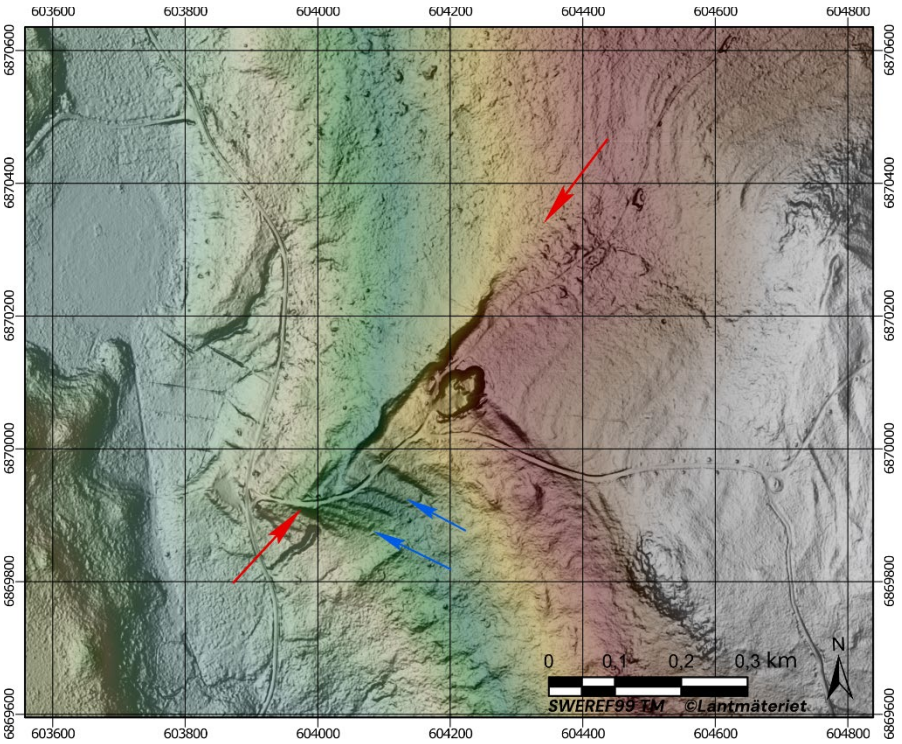

Figure 4-4*. Scarp no. 36 is sharp. The red arrows mark the scarp. On top of the hill, east of the scarp lies a closed sand pit, approximately 10 m deep. The formation is not fully understood, but it is interpreted to be the result of fluvial erosion during relative sea level drop. The area is likely affected by glacial-lake drainages.*

Scarp 246 (Figure 4-5) and 304 are very short scarps that seem to cut shorelines. It is interpreted to be caused by waves deflecting off the bedrock hill.

Scarp 59 and 60 strike approximately N-S and face to the W (Figure 4-6). The main scarp is c. 1 km long. They seemingly crosscut shorelines. Several spring flows are cutting through the scarp line. The interpretation of the scarps is that they formed in a similar way as scarp 36 and 167 – fluvial erosion and wave action during regression.

Scarps 213 and 214 are subtle scarp lines (Figure 4-7), that strikes SW-NE, and face to the SE. After analysis of the paleo-water levels, they are interpreted as a result of wave washing at a shoreline.

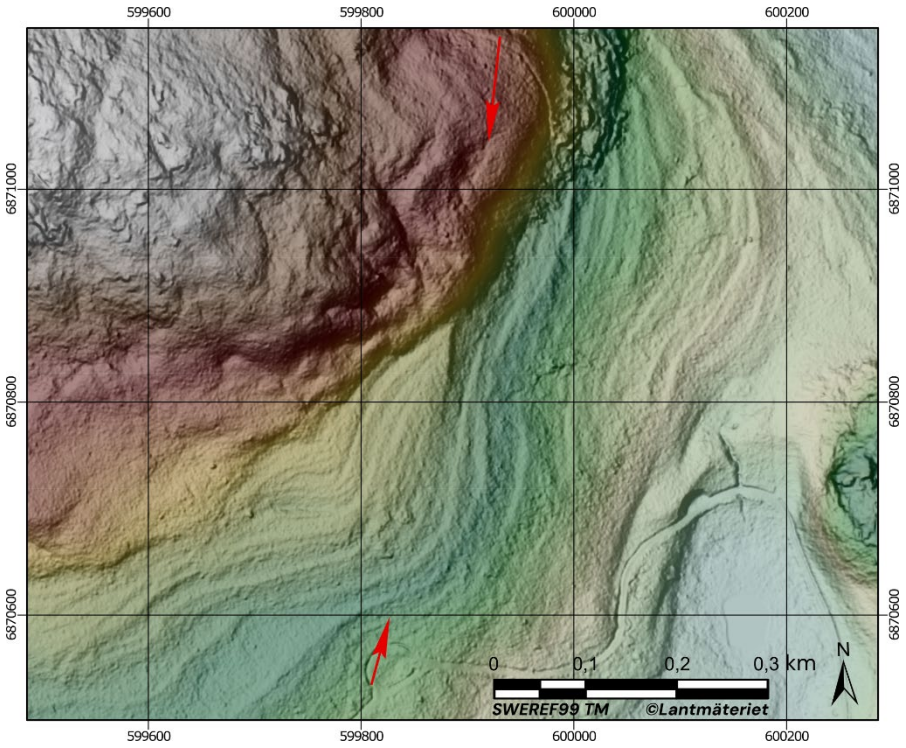

Figure 4-5. *Scarp no. 246 appear to cut shorelines. The cause of appearance is erosion by deflecting waves during isostatic uplift.*

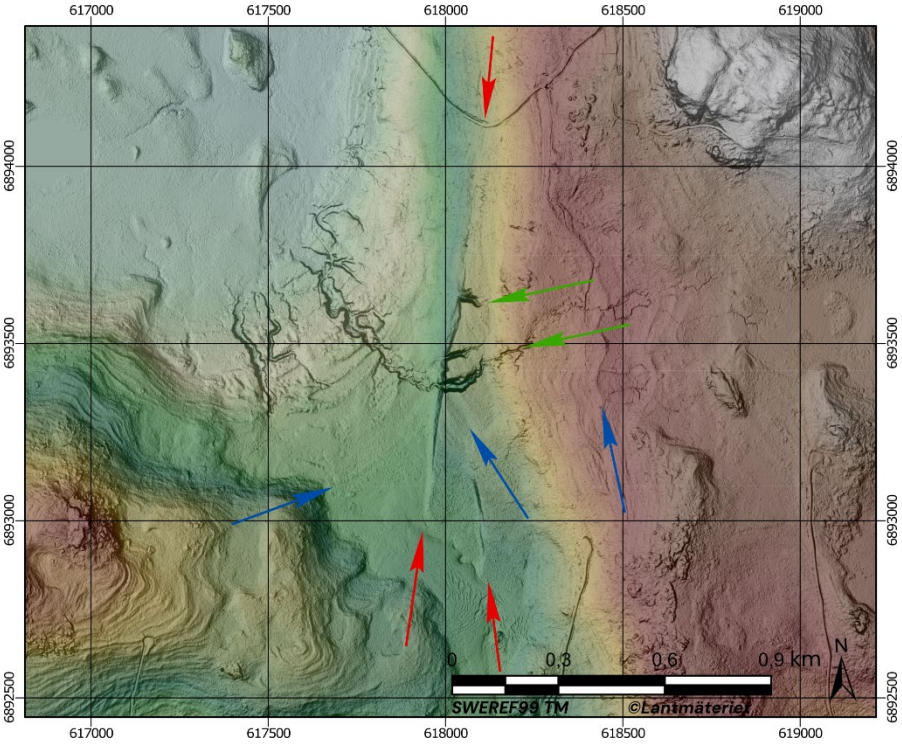

Figure 4-6. *Scarp no. 59 and 60 are sharp with a vertical offset of 10 to 15 m. Green arrows represent spring flows. Shorelines and the scarps are marked by blue and red arrows, respectively.*

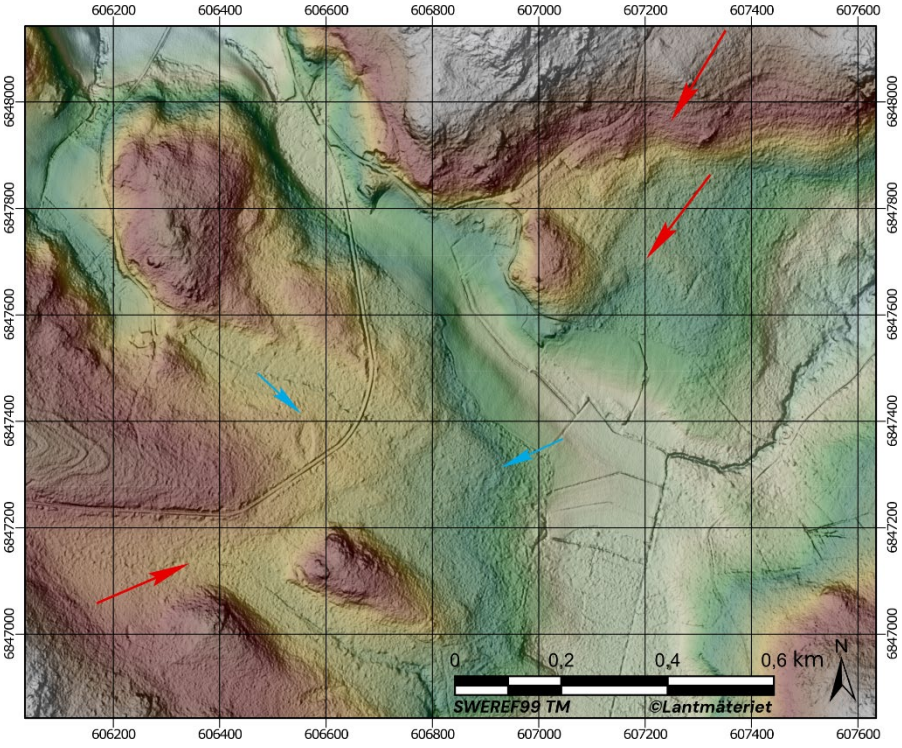

Figure 4-7. *Scarp no 213 and 214 are subtle and are suggested to be related to paleo water levels.*

4.1.2 Bedrock faults without indications of postglacial ruptures

Scarps 252 to 255 form a scarp line parallel to the Bollnäs fault, striking N-S, and faces E (Figure 4-8). They are also parallel to subglacial meltwater features in the area. Field visit reveal that the till cover is thin and patchy in the area. The scarp lines are interpreted to represent old bedrock faults that probably got their final appearance from subglacial meltwater erosion.

Scarps 40 to 45 are a set of N-S trending scarps facing E (Figure 4-9). Scarps are in line with a large fault line that can be followed from near Kramfors to Hudiksvall. The scarps are interesting, but no Quaternary sediment is clearly cut. Bedrock, visible during fieldwork, had c. 5 cm large open fractures at scarp 44 (Figure 4-9). Small-scale faults are reverse, dipping west. The overall interpretation is that they are old bedrock faults, in places highlighted by wave washing. Scarp 43, 2 km south of scarp no. 44, is peculiar and is partly facing west (Figure 4-9 inset). Based on the relation to other landforms, sediment cover, and the other scarps in line with this, it is unclear how they formed. However, within the methodology of this study they cannot regarded as GTF suspects.

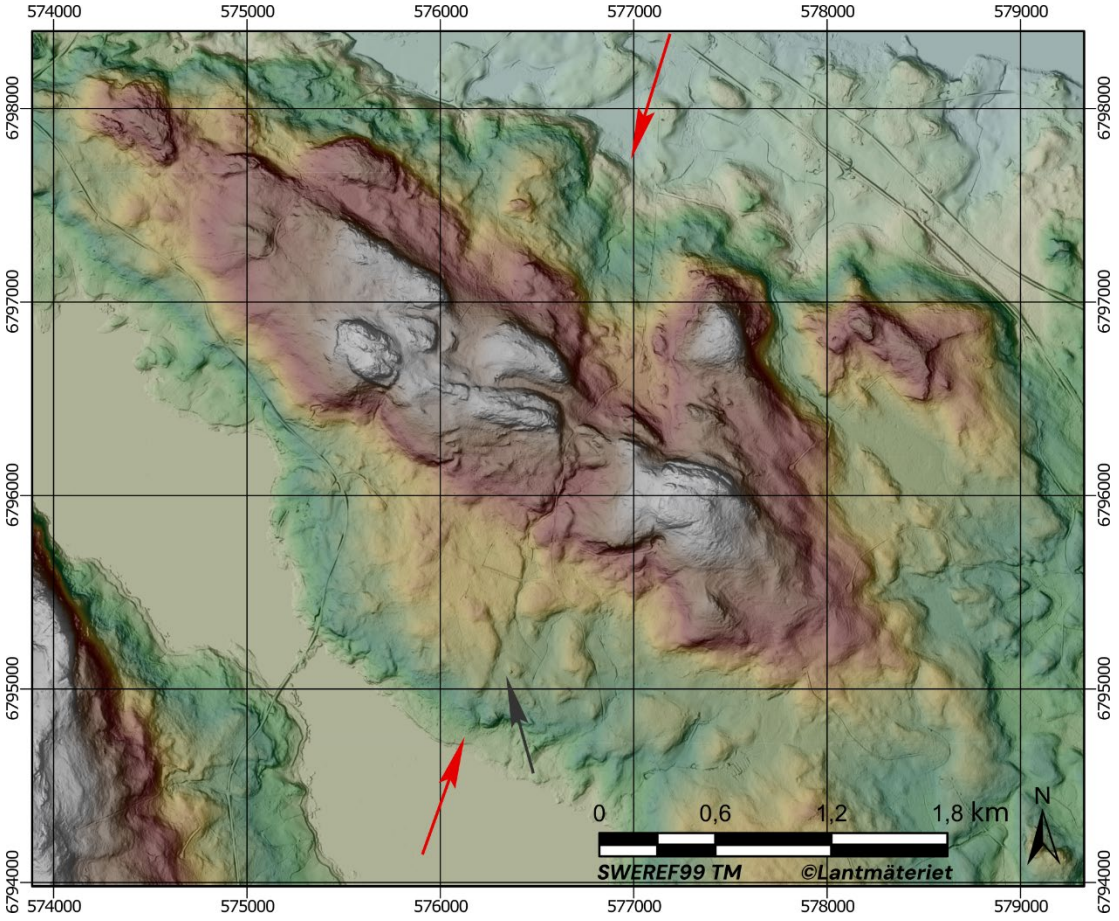

Figure 4-8. *Scarps 252 to 255.*

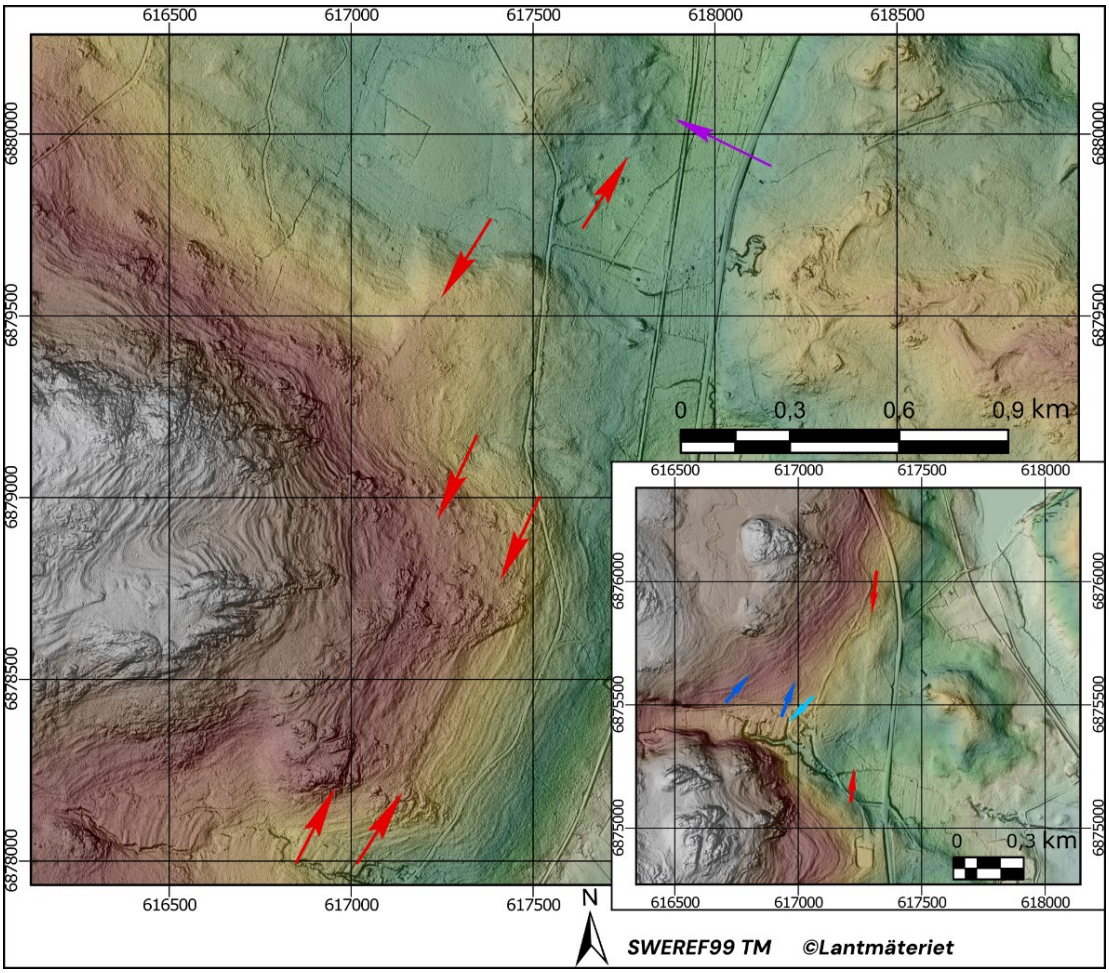

***Figure 4-9**. Scarps no. 44 and 45 are parallel, with unclear origin. Scarp no. 43 (inset) is interesting.*

4.1.3 Subglacial meltwater features

Scarps 200, 201, 202 and 203 extend from a couple of hundred meters to over 2 km in length (Figure 4-10). They have cross cutting orientations in approximately W-E direction and NW-SE. Their appearance and relations to topography and other landforms are typical for subglacial meltwater channels. The scarps are also, either a part of, or related to murtoo landforms in the area. Thus, they are interpreted as subglacial meltwater channels.

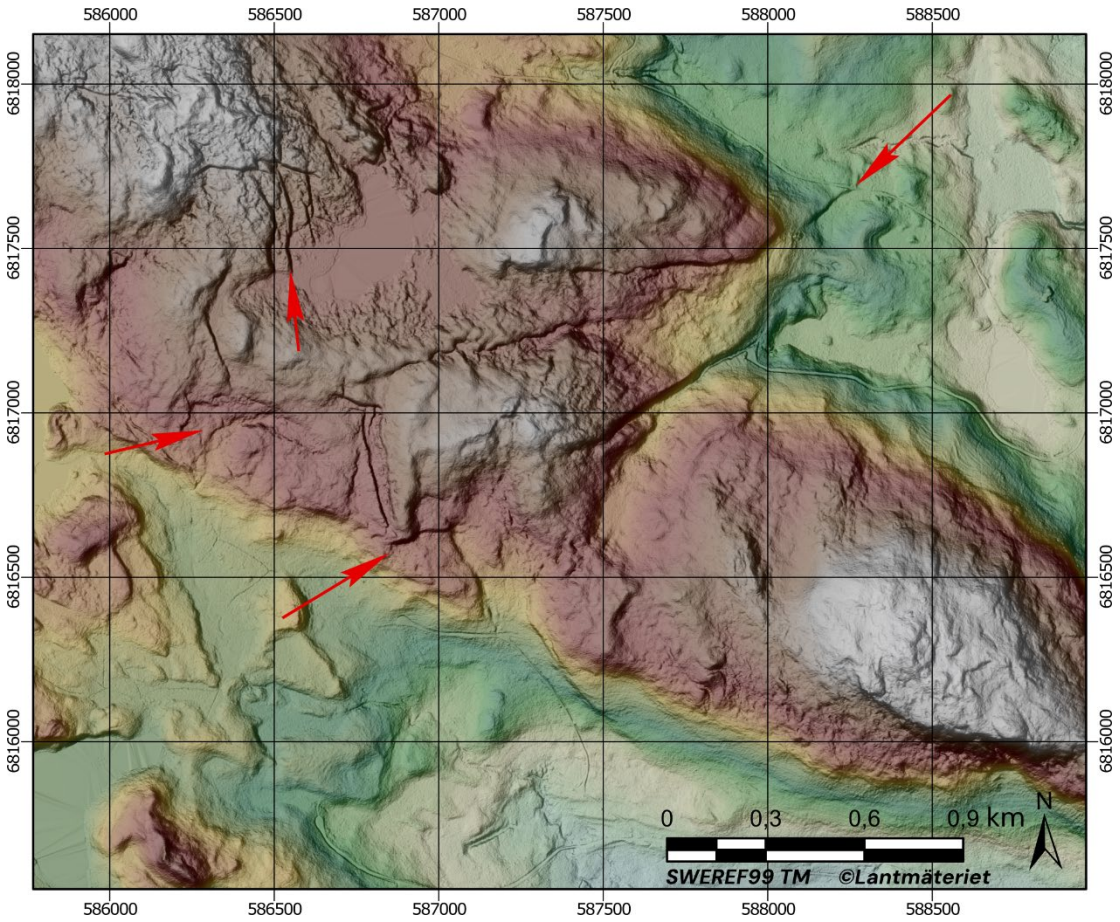

Figure 4-10. *Scarps 200, 201, 202 and 203.*

4.2 Possible GTFs

The origin of the scarps presented below are not clear, the possibility of a postglacial seismic origin cannot be ruled out.

Scarp 7 is a distinct scarp that strikes SW–NE, face towards SE and is 1.2 km long (Figure 4-11). Less than 2 km NE there are large murtoo fields, which could suggest that the scarp has a subglacial meltwater origin. However, the appearance of the scarp and the landscape close by does not indicate a relation to the subglacial meltwater routes. One plausible explanation to the scarp appearance is that it is an old fault scarp covered by thin surficial deposits. However, the glacially induced origin cannot be ruled out.

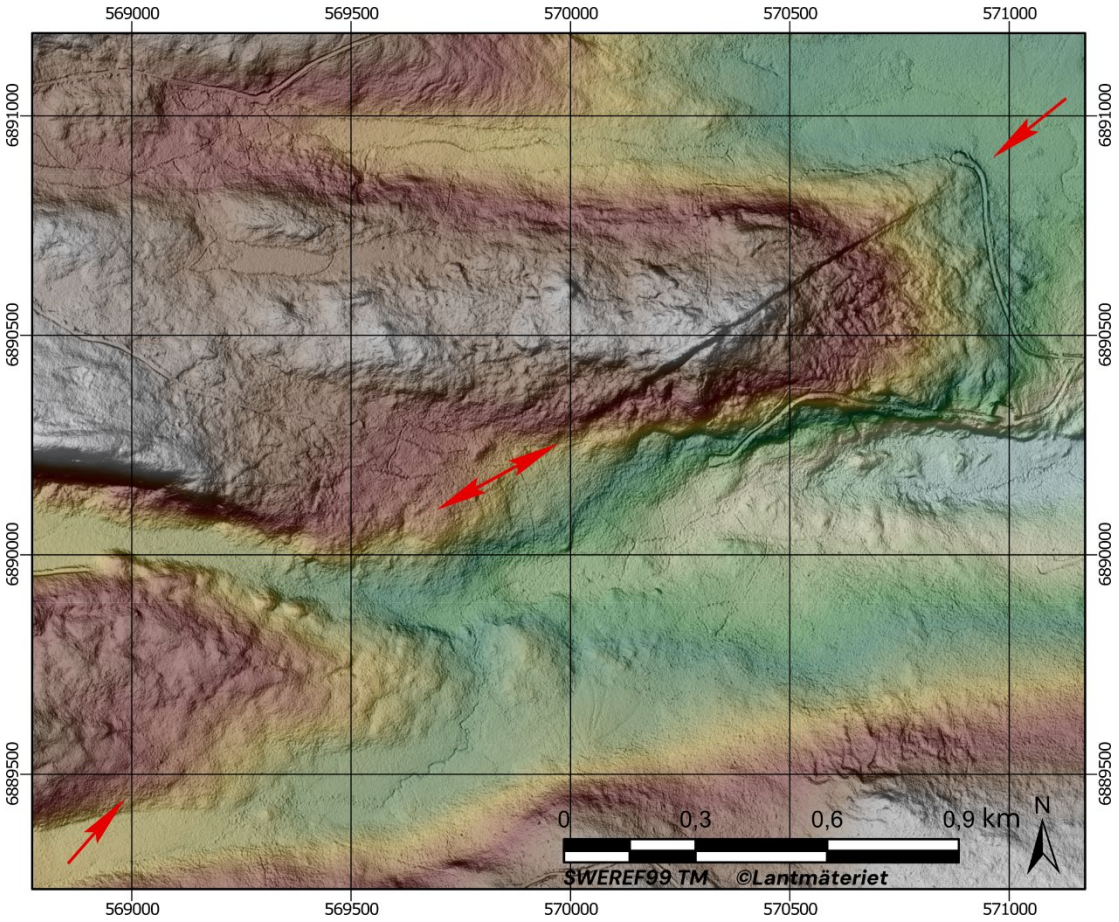

Figure 4-11. *Scarp 7. Note the landslides in the lower right.*

Scarps 192 and 193 are scarps that strike SW-NE and face towards the SE (Figure 4-12). 192 is c. 2 km long and the offset is between 1 and 5 m (Figure 4-12c). Possibly, it is connected to scarp 193 (Figure 4-12a) which is somewhat deflected to the east. Both scarps seem to cut crag and tails. The site was visited during field work. Cannot rule out a glacially induced faulting origin.

Scarps 194,195 and 196 are possibly connected to 192 and 193. They strike SW-NE (SSW-NNE), face towards the SE and have offsets between 4 and 9 m (Figure 4-12b-d). They were visited during fieldwork. These scarps do not crosscut glacial landforms. Preliminarily, they are interpreted to be of subglacial meltwater origin, but the connection to 192 and 193 makes them highly interesting.

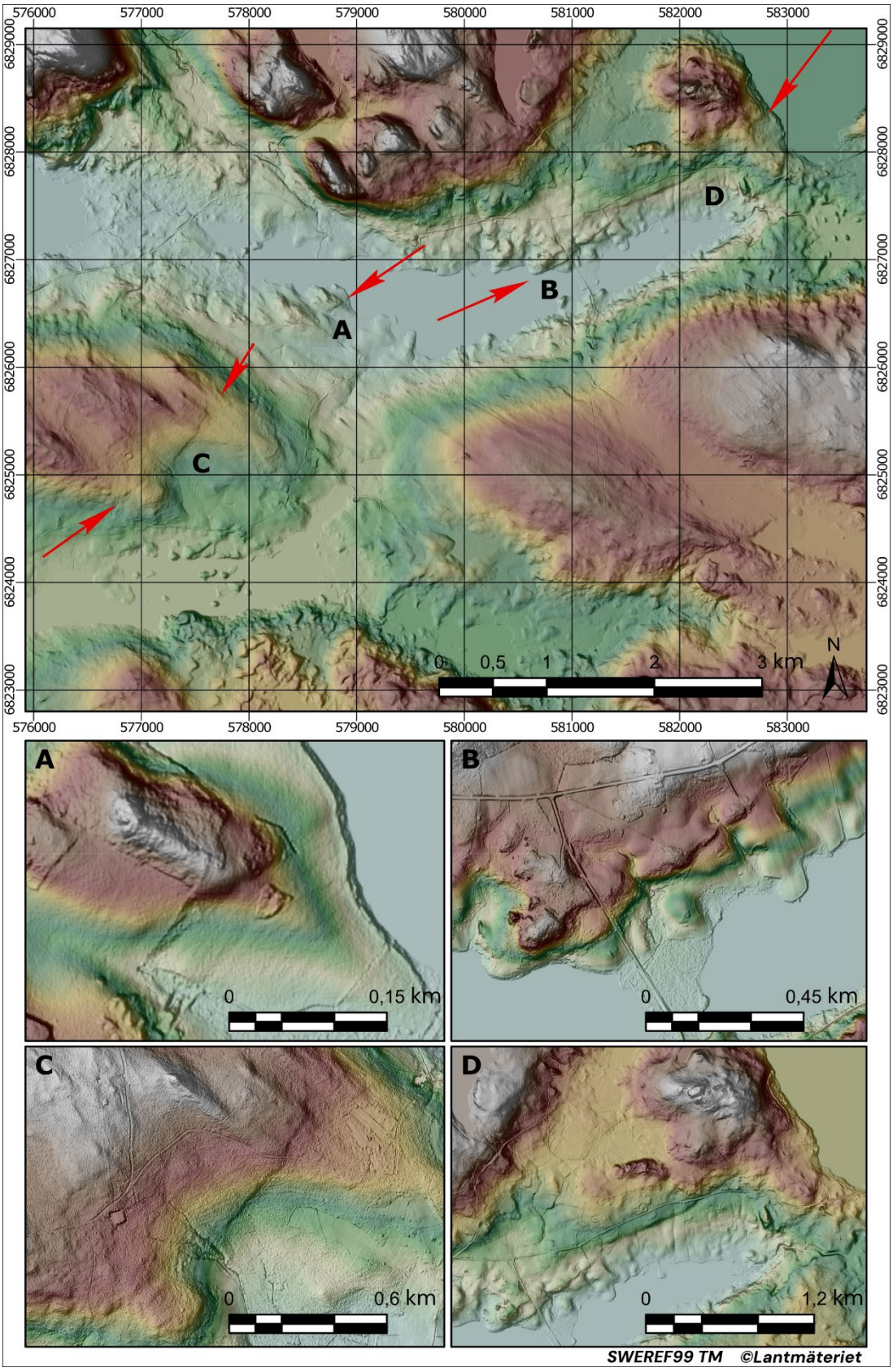

Figure 4-12. *Scarp 192-196.*

Scarp 292 is c. 400 m long and without a clear offset; it rather sticks up (Figure 4-13). The impression is that the surficial deposit depth is thin. The appearance is, however, original and cannot clearly be explained.

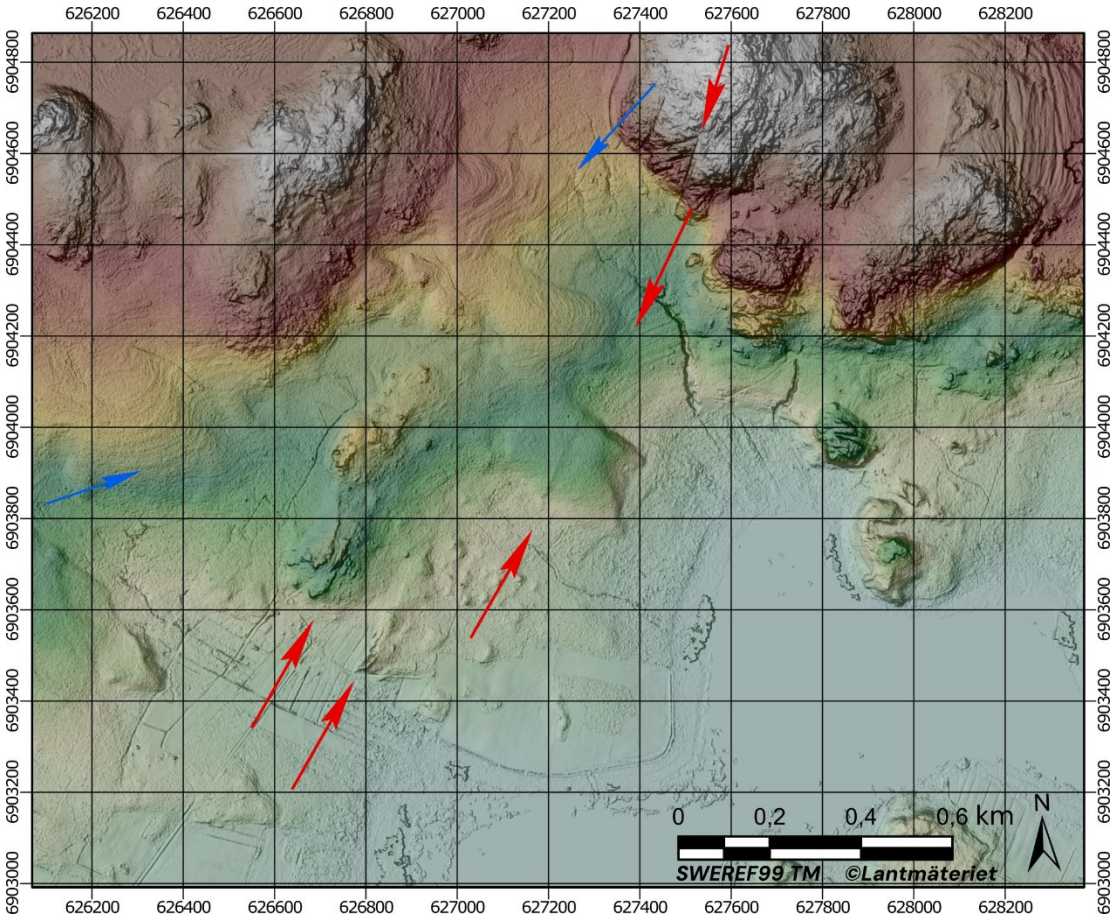

Figure 4-13. *Scarp no 292.*

4.3 Mass movements

The features that are interpreted to represent landslides were identified in the LiDAR imagery as sharp cuts along hill slopes (Figure 4-14). Note that the focus was on scars and scarred slopes and not necessarily to locate a related deposit. The reason for this is that this type of scarred terrain has previously only been noticed in areas with known GTFs.

Over six hundred landslide scars are mapped in this study, besides the seventy scars already in the SGU Database (Figure 4-15a). The majority of the mapped landslide scars are in coarse-grained deposits (most often 'till') and found above or at the highest coastline.

Density analysis of the mapped scars reveals several clusters, depending on chosen tool parameters (Figure 4-15b). Since most landslides related to GIFs in northern Finland occur within 35 km from the epicenter (Ojala et al. 2019a), a 35 km buffered polygon was drawn around the Bollnäs postglacial fault. This shows that the southern cluster(s) is inside the area which may therefore have been caused by the faulting of Bollnäs. Further, this suggests that the mapped landslide scars reveal a northern cluster which lacks an identified, studied fault scarp. Landslides within clusters need to be dated in order to determine if the masses moved in the same time period, and thereby strengthen the idea of an earthquake triggering them. This has successfully been performed at four sites close to Bollnäs (Smith et al. 2014).

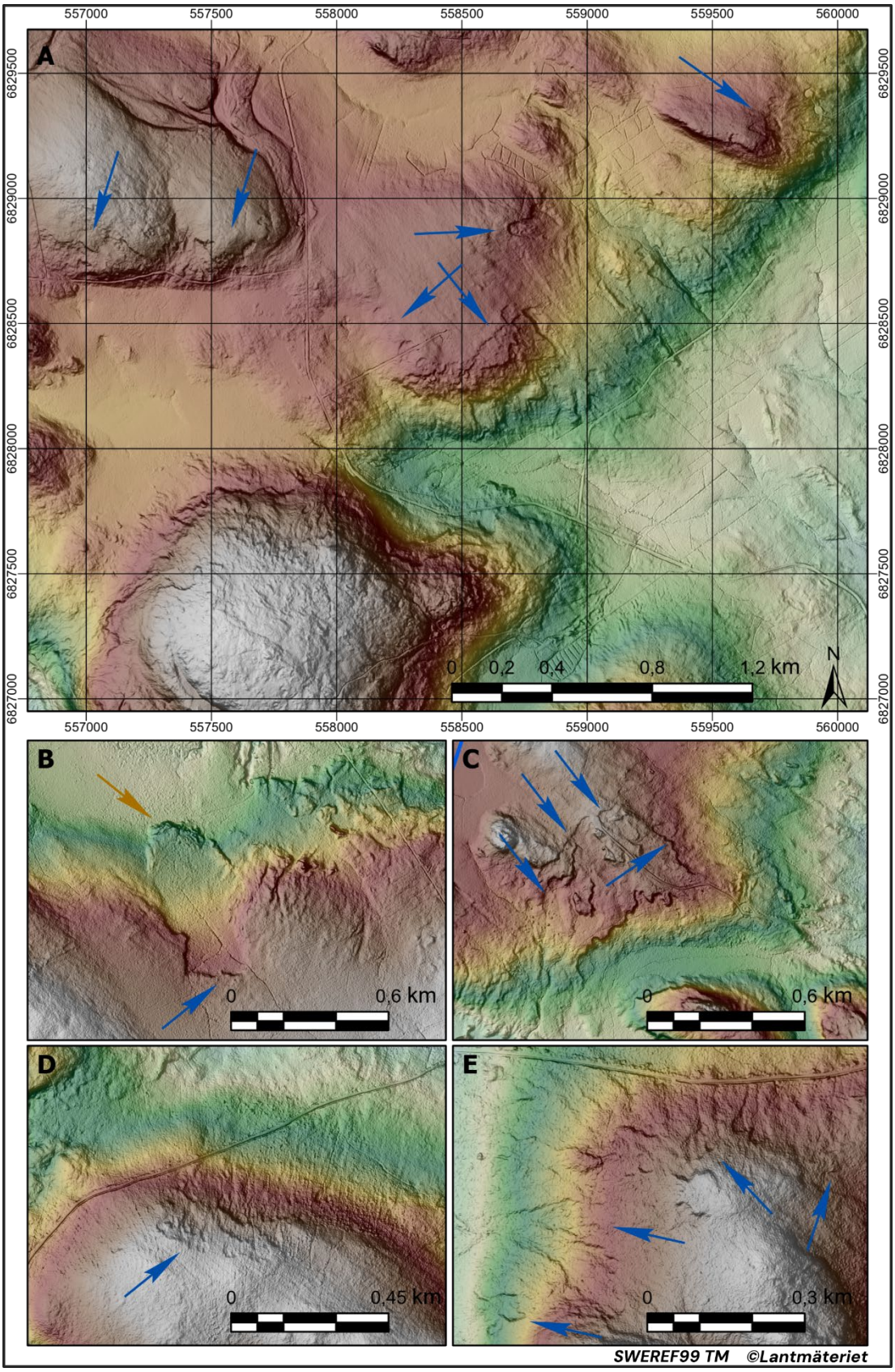

Figure 4-14. *Landslide examples (A-E).*

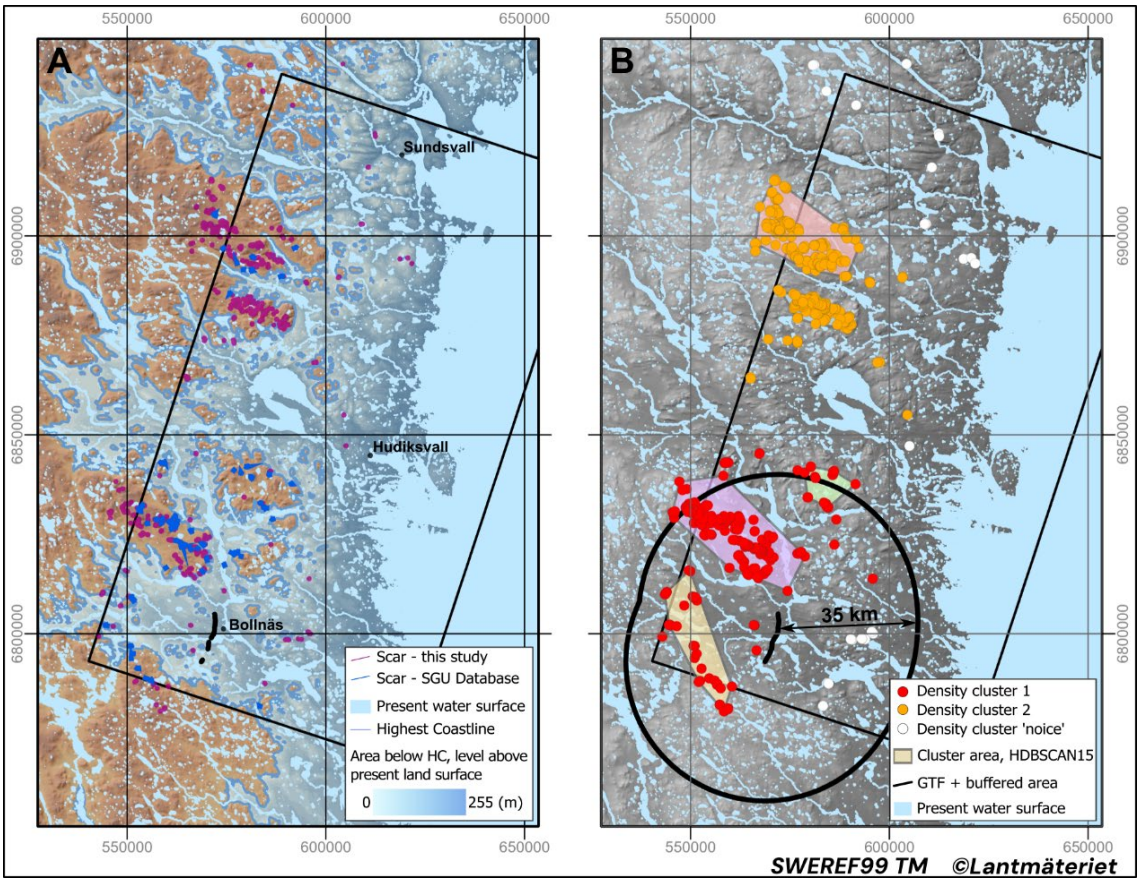

Figure 4-15. *Landslide distribution in the study area. The highest coast line appears to have a large impact on the grade of landslide-scar preservation (A). Landslides represented as points and analyzed with the ArcGIS 'Density Cluster' Tool (B).*

5 Discussion

Three hundred scarp lines are mapped in this study, of which four of the sites are interesting and further investigations are suggested. Thus, the mapping also intends to map linear features which can be mistaken for GTF's but have other origins.

The Bollnäs fault (Malehmir et al. 2016, Mikko et al. 2015, Smith et al. 2014) is the only previously studied and confirmed GTF in the study area. Not shown in the results section are a couple of scarps which appear to represent the continuation of the Bollnäs fault. Though, they do not meet the criteria for GTF's by our remote sensing method.

The scarps presented in Figure 4-11 and 4-12 are very interesting and deserve closer examination. The area around scarp number 7 (Figure 4-11) has a very thin cover of Quaternary deposits, which makes it challenging to excavate a trench as we usually do. However, scarp number 192 and 193 have promising conditions for excavation, and both appear to cross-cut Quaternary sediments and landforms. They are positioned sub-parallel and seem to be connected. Number 193 intersects a crag and tail, while number 192 crosscuts a drumlin and apparently also shoreline features. The scarps are also relatively distinct in the field. The same applies to numbers 194, 195, and 196, which are located northeast of 192 and 193 on the other side of Lake Bysjön. These scarps have a larger vertical offset, than 192-193 and are consequently even more prominent. As described in section 4.2, these have an appearance similar to landforms caused by subglacial erosion. Since the region has abundant traces of subglacial erosion, this type of landform becomes more difficult to interpret. It is the alignment to 192-193 that primarily makes them highly interesting. Secondly, observations have been made, both in the field and in LiDAR images, of bedrock knobs that locally protrudes the surface along the scarps. This suggests that the shape of the landforms is influenced by the bedrock, which is not commonly the case with subglacial erosion features.

In this study, we also mapped over six hundred mass-movement traces, interpreted as landslide scars, not reported before. I suggest this is mainly due to deviating methodology; previous mapping had much more strict criteria regarding which scar features to include. Generally, the SGU Landslide and Ravines Database only includes prominent scars, as in Figure 4-12B, while other examples in Figure 4-12 are excluded.

The mapping has not detected any indisputable new GTFs. However, the surficial appearance of the landscape, which is what has been analysed, has been exposed to various possible erosional processes postglacially (i.e., water, wind, snow, gravitation).

The limit of water-covered areas – the highest coastline – is of great importance since the wave action has affected and redistributed sediment deposits below this elevation. Thus, faults which were possibly reactivated in late- or postglacial times can be impossible to detect with this methodology. Over eighty percent of the study area is situated below the highest coastline, including the parts still under the Baltic Sea surface, accordingly, only a fifth of the area is unaffected by wave washing. Further, scarps can be covered by mass-movement deposits. Mass movements caused by, for example, changing groundwater pore pressures during land uplift, seismicity, or more recent fluvial processes.

5.1 Landslides as indicator

Preserved landslide scars imply a postglacial event origin; otherwise, it likely would have been erased by glacial erosion from the Weichselian Ice Sheet. Figure 4-16 shows that most mapped scars in the area occur above the highest coastline. Wave washing of slopes below this line might prevent detection of once prominent landslide scars.

A few of the mapped scars are at or just below the highest coastline which is a common setting for landslides caused by changing groundwater pore pressures during land uplift (Smith et al. 2017). However, most have not been subjected to this mechanism. The remaining most likely cause for the slope failures are pore pressure changes due to heavy raining (Crosta and Frattini 2008), thawing of permafrost (Lewkowicz and Way 2019) or earthquakes (Jibson 1996).

The abundance and clustering of landslide scars in the southern half of the area are situated within c. 35 km from the Bollnäs Fault and therefore imply a possible correlation. Smith et al. (2014) dated four landslides close to Bollnäs, however, there is a need for further studies and dates in order to understand the appearance and pattern of landslide distribution in connection to the seismicity. Lagerbäck (1990) suggests that the frequency of landslide scars indicate paleo seismic activity in the area.

The paraglacial environment has high sediment yields and denudation rates, which decline with time (Ballantyne and Benn 1994). However, triggered by climate change or extremes, paleo seismicity, or anthropogenic activities, the paraglacial state can be rejuvenated or renewed long after deglaciation (Ballantyne 2014, Curry 2000a, 2000b). Landslides are thus more easily triggered by earthquakes, or other disturbances, shortly after deglaciation and possibly during climatic fluctuations in temperatures and precipitation.

Coarse-grained-sediment landslides are not well documented in Sweden. Although, a nationwide inventory was carried out on LiDAR-based DEM's by the Geological Survey of Sweden in 2014, their criteria were conservative. Thus, there is a need for studies on distribution and morphometry to further categorize and assess how landslides correlate to paleo seismicity.

5.2 Other genesis of fault or fault-like scarps

Subglacial meltwater can shape sharp, straight scarps in the landscape (Figure 4-6). This process is often related to the formation of the glacial landform murtoo (Ojala et al. 2019b). Murtoo related landform scarps can easily be mistaken as GTFs. This was also noted in the previous similar study in the Uppland area (Öhrling et al. 2018).

Scarp no. 288 (Figure 4-2), 167 (Figure 4-3), 36 (Figure 4-4), 246 (Figure 4-5), 59, 60 (Figure 4-6), and more, in supplementary material, are examples of distinct scarps in water-sorted sediments. These have in common that they are interpreted to have been formed by fluvial erosion through wave action, during the relative sea-level drop. By analysing the landscape with regard to past water levels, it is suggested that the scarps in Figure 4-2, 4-4 and 4-6 were formed in association with the closing of sea straits. When the sediment transport changed, the depositional environment changed, and the scarps at these sites were formed.

Thin cover of surficial deposits may inhibit the interpretation of scarps in the landscape surface. Surficial deposits can then falsely appear to be cut by a postglacial fault scarp, albeit much older. However, this type can still be a GTF, yet not from the late Weichselian (c.f. Sutinen and Middleton 2021).

6 Survey suggestions for SKB

This study was a complete desktop study, with the exception of one and a half days of field visits to a few scarps. To assess whether the identified scarps in section 4.2 are GTFs, firstly, they need to be examined in the field.

6.1 Suggestions for field investigation

The proposition is a campaign composed of a field-reconnaissance part to evaluate the scarps by visual inspection and to identify suitable sites for trenching. Further, it is suggested to excavate trenches, c. 30 m long, at the selected sites, to confirm or refute the faulting origin of these features. In the trench cuts, we recommend detailed till-stratigraphy surveys with focus on textures, lithostratigraphy, structures, geochemistry, and clast fabric. More specifically, the suggestions are:

- A field visit to scarp 7 (Figure 4-11) which is needed to assess further actions. A road crosses the scarp at the northern end, which suggests easy access.
- Scarps 192 and 193 (Figure 4-12c) meet several criteria for GTF and would be reasonable to trench. A field visit by car in 2020 used a road that crosses the 192 scarp and would be suitable to use in order to access with an excavator.
- Scarps 194 to 196 (Figure 4-12b-d) are highly interesting based on the possible relation to scarps 192 and 193. There are a couple of suitable sites where access with excavator is easy.

6.2 Suggestions for further studies

Below are a few proposals for follow-up:

- Documentation of sand sections in gravel pits in search of soft-sediment deformation structures. Some of the examples in section 4.1 could be candidates for this. Further, there are many more gravel pits in the study area that would be included in a preparatory GIS analysis to select appropriate sites.
- Core basins of sediment and/or peat covered by landslide deposits, in order to recover organic material for carbon-14 dating of maximum ages of the landslides.
- National mapping of landslides, primarily, in coarse-grained sediments, assisted by AI-techniques. Morphometric and distributional analysis in order to classify the landslide scars by its properties.

7 Acknowledgement

State geologists Colby Smith and Henrik Mikko are here deeply acknowledged for discussing the work and generously offer their time to improve the manuscript. Additional thanks to Colby for helping with the English language and partnering up in the field. Former state geologist, Susanne Grigull at SKB is also thanked for constructive criticism and ideas. Also, Susanne and state geologist Stefan Bergman greatly improved the section on bedrock geology. Lastly, Jenny Gåling and Juri Palmtag at SKB are thanked for the final review.

References

SKB's (Svensk Kärnbränslehantering AB) publications can be found at www.skb.com/publications.

Agrell H, 1981. Gillberga gryt - en sentida sprickgrotta i Uppland. Grottan 4, 28–29. (in Swedish.)

Ahjos T, Uski M, 1992. Earthquakes in northern Europe in 1375-1989. Tectonophysics 207, 1–23. https://doi.org/10.1016/0040-1951(92)90469-M

Andrén T, Björck S, Andrén E, Conley D, Zillén L, Anjar J, 2011. The development of the Baltic Sea basin during the dast 130 ka. In Harff J, Björck S, Hoth P (eds). The Baltic Sea basin: Central and eastern European development studies (CEEDES), 75–97. Heidelberg, Belin: Springer. https://doi.org/10.1007/978-3-642-17220-5_4

Ballantyne C K, 2014. Paraglacial landsystems. In Evans D, Glacial Landsystems. 2014 (ed). London: Routledge. https://doi.org/10.4324/9780203784976

Ballantyne C K, Benn D I, 1994. Paraglacial slope adjustment and resedlmenfation following recent glacier retreat, Fåbergstølsdalen, Norway. Arctic and Alpine Research 26, 255–269. https://doi.org/10.1080/00040851.1994.12003065

Berglund M, 2004. Holocene shore displacement and chronology in Ångermanland, eastern Sweden, the Scandinavian glacio-isostatic uplift centre. Boreas 33, 48–60. https://doi.org/10.1111/j.1502-3885.2004.tb00995.x

Berglund M, 2005. The Holocene shore displacement of Gästrikland, eastern Sweden: A contribution to the knowledge of Scandinavian glacio-isostatic uplift. Journal of Quaternary Science 20, 519–531. https://doi.org/10.1002/jqs.928

Bergman S, Sjöström H, 1994. The Störsjon-Edsbyn Deformation Zone, central Sweden [Research report]. Uppsala University.

Bergman S, Sjöström H, Högdahl K, 2006. Transpressive shear related to arc magmatism: The Paleoproterozoic Storsjön-Edsbyn Deformation Zone, central Sweden. Tectonics 25. https://doi.org/10.1029/2005TC001815

Bergman S, Stephens M B, Andresson J, Kathol B, Bergman T, 2012. Sveriges berggrund, skala 1:1 miljon. K 423, Sveriges geologiska undersökning. (In Swedish.)

Carlsten S, Stråhle A, 2000. Borehole radar and BIPS investigations in boreholes at the Boda area. Available at: https://www.osti.gov/etdeweb/biblio/20153359

Crosta G B, Frattini P, 2008. Rainfall-induced landslides and debris flows. Hydrological Processes 22, 473–477. https://doi.org/10.1002/hyp.6885

Curry A M, 2000a. Holocene reworking of drift-mantled hillslopes in the Scottish Highlands. Journal of Quaternary Science 15, 529–541. https://doi.org/10.1002/1099-1417(200007)15:5<529::AID-JQS531>3.0.CO;2-D

Curry A M, 2000b. Observations on the distribution of paraglacial reworking of glacigenic drift in western Norway. Norsk Geografisk Tidsskrift - Norwegian Journal of Geography 54, 139–147. https://doi.org/10.1080/002919500448512

Dai F C, Lee C F, Wang S J, 2003. Characterization of rainfall-induced landslides. International Journal of Remote Sensing 24, 4817–4834. https://doi.org/10.1080/01431160131000082424

De Geer G, 1929. Den finiglaciala landisrecessionen i Gävletrakten. Geologiska Föreningens i Stockholm Förhandlingar 51, 566–572. (In Swedish.) https://doi.org/10.1080/11035892909449567

Douglas T A, Hiemstra C A, Anderson J E, Barbato R A, Bjella K L, Deeb E J, Gelvin A B, Nelsen P E, Newman S D, Saari S P, Wagner A M, 2021. Recent degradation of interior Alaska permafrost mapped with ground surveys, geophysics, deep drilling, and repeat airborne lidar. The Cryosphere, 15, 3555–3575. https://doi.org/10.5194/tc-15-3555-2021

Farquharson L M, Romanovsky V E, Cable W L, Walker D A, Kokelj S V, Nicolsky D, 2019. Climate change drives widespread and rapid thermokarst development in very cold permafrost in the Canadian High Arctic. Geophysical Research Letters 46, 6681–6689. https://doi.org/10.1029/2019GL082187

Greenwood S L, Clason C C, Mikko H, Nyberg J, Peterson G, Smith C A, 2015. Integrated use of LiDAR and multibeam bathymetry reveals onset of ice streaming in the northern Bothnian Sea. GFF 137, 284–292. https://doi.org/10.1080/11035897.2015.1055513

Greenwood S L, Clason C C, Nyberg J, Jakobsson M, Holmlund P, 2017. The Bothnian Sea ice stream: Early Holocene retreat dynamics of the south-central Fennoscandian Ice Sheet. Boreas 46, 346–362. https://doi.org/10.1111/bor.12217

Grigull S, Peterson G, Nyberg J, Öhrling C, 2019. Phanerozoic faulting of Precambrian basement in Uppland. SKB R-19-22, Svensk Kärnbränslehantering AB.

Grånäs K, 2010. Beskrivning till jordartskartan delar av Sundsvalls kommun. Sveriges Geologiska Undersökning, K261. (In Swedish.) Available at: www.sgu.se

Haapaniemi, A I, Scourse J D, Peck V L, Kennedy H, Kennedy P, Hemming S R, Furze M F A, Pienkowski A J, Austin W E N, Walden J, Wadsworth E, Hall I R, 2010. Source, timing, frequency and flux of ice-rafted detritus to the Northeast Atlantic margin, 30–12 ka: Testing the Heinrich precursor hypothesis. Boreas 39, 576–591. https://doi.org/10.1111/J.1502-3885.2010.00141.X

Hall A M, Krabbendam M, Van Boeckel M, Goodfellow B W, Hättestrand C, Heyman J, Palamakumbura R N, Stroeven A P, Näslund J-O, 2020. Glacial ripping: Geomorphological evidence from Sweden for a new process of glacial erosion. Geografiska Annaler: Series A, Physical Geography 102, 333–353. https://doi.org/10.1080/04353676.2020.1774244

Hanson K L, Kelson K I, Angell M A, Lettis W R, 1999. Techniques for identifying faults and determining their origins. NUREG/CR-5, U.S. Nuclear Regulatory Commission Office of Nuclear Regulatory Research, United States.

Heidbach O, Rajabi M, Reiter K, Ziegler M, WSM Team, 2016. World Stress Map Database Release 2016. Version 1.1. GFZ Data Services. https://doi.org/10.5880/WSM.2016.001

Heinrich H, 1988. Origin and consequences of cyclic ice rafting in the Northeast Atlantic Ocean during the past 130,000 years. Quaternary Research 29, 142–152. https://doi.org/10.1016/0033-5894(88)90057-9

Hemming S R, 2004. Heinrich events: Massive late Pleistocene detritus layers of the North Atlantic and their global climate imprint. Reviews of Geophysics 42. https://doi.org/10.1029/2003RG000128

Hughes A L C, Gyllencreutz R, Lohne Ø S, Mangerud J, Svendsen J I, 2016. The last Eurasian ice sheets: A chronological database and time-slice reconstruction, DATED-1. Boreas 45, 1–45. https://doi.org/10.1111/bor.12142

Hunt A G, Malin P E, 1998) Possible triggering of Heinrich events by ice-load-induced earthquakes. Nature 393, 155–158. https://doi.org/10.1038/30218

Högdahl K, Bergman S, 2020. Paleoproterozoic (1.9-1.8 Ga), syn-orogenic magmatism and sedimentation in the Ljusdal lithotectonic unit, Svecokarelian orogen. In Stephens M B, Bergman WeihedJ, Sweden: Lithotectonic Framework, Tectonic Evolution and Mineral Resources. 2020 (ed). Memoirs 50, 131–153. London: Geological Society. https://doi.org/10.1144/M50-2016-30

Högdahl K, Sjöström H, Bergman S, 2009. Ductile shear zones related to crustal shortening and domain boundary evolution in the central Fennoscandian Shield. Tectonics 28. https://doi.org/10.1029/2008TC002277

Jibson R W, 1996. Use of landslides for paleoseismic analysis. Engineering Geology 43, 291–323. https://doi.org/10.1016/S0013-7952(96)00039-7

Jibson R W, 2012. Models of the triggering of landslides during earthquakes. In Clague J J, Stead D, Landslides: Types, Mechanisms and Modeling. 2012 (eds). Cambridge: Cambridge University Press, 196–206. https://doi.org/10.1017/CBO9780511740367.018

Karlsson C, Sohlenius G, Becher G P, 2021. Handledning för jordartsgeologiska kartor och databaser över Sverige. 2021:17, Sveriges geologiska undersökning, 1–83. (In Swedish.)

Keefer D K, 1984. Landslides caused by earthquakes. Geological Society of America Bulletin 95, 406–421. https://doi.org/10.1130/0016-7606(1984)95<406:LCBE>2.0.CO;2

Keefer D K, 2002. Investigating landslides caused by earthquakes: A historical review. Surveys in Geophysics 23, 473–510.

Kujansuu R, 1972. On landslides in Finnish Lapland. Geological Survey of Finland Bulletin 256, 1–23.

Lagerbäck R, 1990. Late Quaternary faulting and-paleoseismicity in northern Fennoscandia, with particular reference to the Lansjärv area, northern Sweden. GFF 112, 333–354. https://doi.org/10.1080/11035899009452733

Lagerbäck R, Sundh M, 2008. Early Holocene faulting and paleoseismicity in northern Sweden. Research Papers C836, Sveriges geologiska undersökning. http://books.google.se/books?id=Dql9PgAACAAJ

Lagerbäck R, Sundh M, Svedlund J-O, Johansson H, 2005. Forsmark site investigation. Searching for evidence of late-or postglacial faulting in the Forsmark region. SKB R-05-51, Svensk Kärnbränslehantering AB.

Lantmäteriet, 2021. Terrain Model Download, grid 1+ (p. 8). Gävle: Lantmäteriet.

Lewkowicz A G, Way R G, 2019. Extremes of summer climate trigger thousands of thermokarst landslides in a High Arctic environment. Nature Communications 10. https://doi.org/10.1038/s41467-019-09314-7

Lidmar-Bergström K, Olvmo M, 2015. Plains, steps, hilly relief and valleys in northern Sweden: Review, interpretations and implications for conclusions on Phanerozoic tectonics. Research Papers C838, Sveriges geologiska undersökning.

Lissak C, Bartsch A, De Michele M, Gomez C, Maquaire O, Raucoules D, Roulland T, 2020. Remote sensing for assessing landslides and associated hazards. Surveys in Geophysics 41, 1391–1435. https://doi.org/10.1007/s10712-020-09609-1

Lund B, Roberts R, Smith C A, 2017. Review of paleo-, historical and current seismicity in Sweden and surrounding areas with implications for the seismic analysis underlying SKI report 92:3 2017:35. SKI Report 2017:35, Statens strålskyddsinstitut (Swedish Radiation Protection Authority).

Lund B, Schmidt P, Hossein Shomali Z, Roth M, 2021. The modern Swedish National Seismic Network: Two decades of intraplate microseismic observation. Seismological Research Letters 92, 1747–1758. https://doi.org/10.1785/0220200435

Lundqvist J, 1963. Beskrivning till jordartskarta över Gävleborgs län. Ca 42, Sveriges Geologiska Undersökning. (In Swedish.)

Malehmir A, Andersson M, Mehta S, Brodic B, Munier R, Place J, Maries G, Smith C A, Kamm J, Bastani M, Mikko H, Lund B, 2016. Post-glacial reactivation of the Bollnäs fault, central Sweden: A multidisciplinary geophysical investigation. Solid Earth 7, 509–527. https://doi.org/10.5194/se-7-509-2016

Mangerud J, Birks H H, Halvorsen L S, Hughes A L C, Nashoug O, Nystuen J P, Paus A, Sørensen R, Svendsen J I, 2018. The timing of deglaciation and sequence of pioneer vegetation at Ringsaker, eastern Norway: And an earthquake-triggered landslide. Norwegian Journal of Geology 98, 315–332. https://doi.org/10.17850/njg98-3-03

Mark D F, Lindgren P, Fallick A E, 2013. A high-precision 40Ar/39Ar age for hydrated impact glass from the Dellen impact, Sweden. Geological Society Special Publication 378, 349–366. https://doi.org/10.1144/SP378.22

Mikko H, Smith C A, Lund B, Ask M V S, Munier R, 2015. LiDAR-derived inventory of post-glacial fault scarps in Sweden. GFF 137, 1–5. https://doi.org/10.1080/11035897.2015.1036360

Moon S, Perron J T, Martel S J, Goodfellow B W, Mas Ivars D, Hall A, Heyman J, Munier R, Näslund J-O, Simeonov A, Stroeven A P, 2020. Present-day stress field influences bedrock fracture openness deep into the subsurface. Geophysical Research Letters 47, e2020GL090581. https://doi.org/10.1029/2020GL090581

Munier R, Adams J, Brandes C, Brooks G, Dehls J, Einarsson P, Gibbons S J, Hjartardóttir Á R, Hogaas F, Johansen T A, Kvaerna T, Mattila J, Mikko H, Müller K, Nikolaeva S B, Ojala A, Olesen O, Olsen L, Palmu J-P, Tassis G, 2020. International database of Glacially Induced Faults. PANGAEA. Available at: https://doi.org/10.1594/PANGAEA.922705

Mörner N-A, 1996. Liquefaction and varve disturbance as evidence of paleoseismic events and tsunamis: The autumn 10,430 BP event in Sweden. Quaternary Science Revue 15, 939–948. https://doi.org/10.1016/S0277-3791(96)00057-1

Mörner N-A, 1999. Paleo-tsunamis in Sweden. Physics and Chemistry of the Earth, Part B: Hydrology, Oceans and Atmosphere 24, 443–448. https://doi.org/10.1016/S1464-1909(99)00026-X

Mörner N-A, 2003. Paleoseismicity of Sweden - a novel paradigm. Nils-Axel Mörner Paleogeophysics & Geodynamics. ISBN: 91-631-4072-1.

Mörner N-A, 2004. Active faults and paleoseismicity in Fennoscandia, especially Sweden. Primary structures and secondary effects. Tectonophysics 380, 139–157. https://doi.org/10.1016/j.tecto.2003.09.018

Mörner N-A, 2011. Paleoseismology: The application of multiple parameters in four case studies in Sweden. Quaternary International 242, 65–75. https://doi.org/10.1016/j.quaint.2011.03.054

Mörner N-A, 2013. Patterns in seismology and palaeoseismology, and their application in long-term hazard assessments - The Swedish case in view of nuclear waste management. Pattern Recognition in Physics 1, 75–89. https://doi.org/10.5194/prp-1-75-2013

Mörner N-A, Sjöberg R, 2018. Merging the concepts of pseudokarst and paleoseismicity in Sweden: A unified theory on the formation of fractures, fracture caves, and angular block heaps. International Journal of Speleology 47. https://doi.org/10.5038/1827-806X.47.3.2225

Ojala A E K, Markovaara-Koivisto M, Middleton M, Ruskeeniemi T, Mattila J, Sutinen R, 2018) Dating of paleolandslides in western Finnish Lapland. Earth Surface Processes and Landforms 43, 2449–2462. https://doi.org/10.1002/esp.4408

Ojala A E K, Mattila J, Markovaara-Koivisto M, Ruskeeniemi T, Palmu J-P, Sutinen R, 2019a. Distribution and morphology of landslides in northern Finland: An analysis of postglacial seismic activity. Geomorphology 326, 190–201. https://doi.org/10.1016/j.geomorph.2017.08.045

Ojala A E K, Peterson G, Mäkinen J, Johnson M D, Kajuutti K, Palmu J P, Ahokangas E, Öhrling C, 2019b. Ice-sheet scale distribution and morphometry of triangular-shaped hummocks (murtoos): A subglacial landform produced during rapid retreat of the Scandinavian Ice Sheet. Annals of Glaciology 60, 115–126. https://doi.org/10.1017/aog.2019.34

Olsen L, Olesen O, Høgaas F, 2021. A part of the Stuoragurra postglacial fault complex, at Máze in N-Norway, is less than 600 yrs old. In Nakrem H A, Husås A M, Abstracts and Proceedings of the Geological Society of Norway: The 34th Nordic Geological Winter Meeting 1. 2020 (eds). Digitally, 6–8 January, 2020.

Oinonen K, Uski M, Soosalu H, 2021. FENCAT(2021): Fennoscandian earthquake catalogue [Data set]. Institute of Seismology**,** University of Helsinki. https://doi.org/10.23729/8fe15ab2-e805-447c-934e-21cb0463414b

QGIS.org, 2022. QGIS Geographic Information System. Beaverton, OR: Open Source Geospatial Foundation.

Sandersen P B E, Sutinen R, 2021. Earthquake-induced landforms in the context of ice-sheet loading and unloading. In Steffen H, Olesen O, Sutinen R, Glacially-Triggered Faulting. 2021 (eds). Cambridge: Cambridge University Press, 43–66. https://doi.org/10.1017/9781108779906.006

SGU, 2022. Bedrock 1:1 M. Geological Survey of Sweden.

Sjöberg R, 1986. Caves indicating neotectonic activity in Sweden. Geografiska Annaler: Series A, Physical Geography 68, 393–398. https://doi.org/10.1080/04353676.1986.11880189

Sjöström H, Högdahl K, Aaro S, Bergman S, 2000. The Hassela Shear Zone in central Sweden, the western part of a paleo-Proterozoic tectonic domain boundary across the Baltic Shield? In Eide E, Nordiske Geologiske Vintermøte, Trondheim, Abstract Volume 24, 153.

Skyttä P, Weihed P, Högdahl K, Bergman S, Stephens M B, 2020. Paleoproterozoic (2.0–1.8 Ga) syn-orogenic sedimentation, magmatism and mineralization in the Bothnia–Skellefteå lithotectonic unit, Svecokarelian orogen. In Stephens M B, Bergman Weihed J, Sweden: Lithotectonic Framework, Tectonic Evolution and Mineral Resources. 2020 (eds). London: Geological Society, Memoirs 50, 83–130. https://doi.org/10.1144/M50-2017-10

Slaymaker O, 2009. Proglacial, periglacial or paraglacial? In Knight J, Harrison S, Periglacial and paraglacial processes and environments. 2009 (eds). London: Geological Society, Special Publications 320, 71–84. https://doi.org/10.1144/SP320.6

Smith C A, Öhrling C, 2022. Assessing the validity of proposed paleo-tsunami deposits in Sweden. Quaternary Science Reviews 298, 107849. https://doi.org/10.1016/J.QUASCIREV.2022.107849

Smith C A, Sundh M, Mikko H, 2014. Surficial geology indicates early Holocene faulting and seismicity, central Sweden. International Journal of Earth Sciences 103, 1711–1724. https://doi.org/10.1007/s00531-014-1025-6

Smith C A, Larsson O, Engdahl M, 2017. Early Holocene coastal landslides linked to land uplift in western Sweden. Geografiska Annaler: Series A, Physical Geography, 288–311. https://doi.org/10.1080/04353676.2017.1329624

Steffen H, Olesen O, Sutinen R (eds), 2021. Glacially-Triggered Faulting. Cambridge: Cambridge University Press.

Stewart I S, Sauber J, Rose J, 2000. Glacio-seismotectonics: Ice sheets, crustal deformation and seismicity. Quaternary Science Reviews 19, 1367–1389. https://doi.org/10.1016/S0277-3791(00)00094-9

Strömberg B, 1989. Late Weichselian deglaciation and varve chronology in East-Central Sweden. Ca 73, Sveriges geologiska undersökning.

Sutinen R, Middleton M, 2021. Porttipahta end moraine in Finnish Lapland is constrained to Early Weichselian (MIS 5d, Herning stadial). Geomorphology 393, 107942. https://doi.org/10.1016/j.geomorph.2021.107942

Sutinen R, Piekkari M, Middleton M, 2009. Glacial geomorphology in Utsjoki, Finnish Lapland proposes Younger Dryas fault-instability. Global and Planetary Change 69, 16–28. https://doi.org/10.1016/j.gloplacha.2009.07.002

Varnes D J, 1978. Slope movement types and processes. In Schuster R L, Krizek R J, Landslides: Analysis and control. 1978 (eds). Special Report 176. Washington, D.C.: Transportation Research Board, National Academy of Science, 11–33.

Wänstedt S, 2000. Geophysical and geological investigations of the Boda area. SKB R-00-23, Svensk Kärnbränslehantering AB.

Öhrling C, Peterson G, Mikko H, 2018. Detailed geomorphological analysis of LiDAR derived elevation data, Forsmark Searching for indicatives of late-and postglacial seismic activity. SKB R-18-10, Svensk Kärnbränslehantering AB.

Öhrling C, Peterson G, Sohlenius G, Mikko H, 2019. Iceberg scouring in terrestrial eastern Sweden and implications for deglacial history. 20th Congress of the International Union for Quaternary Research (INQUA). https://app.oxfordabstracts.com/events/574/program-app/submission/94251

Supplementary material (deliveries)

ESRI file geodatabase with mapped scarps and mass-movement scars.